ANALYSIS OF VAPOR BARRIER EXPERIMENTS TO EVALUATE THEIR EFFECTIVENESS AS A MEANS TO MITIGATE HF CONCENTRATIONS

by

Robert N. Meroney
David E. Neff
Seong-Hee Shin
Thomas C. Steidle
Thomas Z. Tan
Gang Wu

FLUID MECHANICS AND WIND ENGINEERING PROGRAM

CER88-89RNM-DEN-SHS-TS-TZT-GW-1

Colorado State University

ANALYSIS OF VAPOR BARRIER EXPERIMENTS TO EVALUATE THEIR EFFECTIVENESS AS A MEANS TO MITIGATE HF CLOUD CONCENTRATIONS

FINAL REPORT

(April 1988 - June 1988)

by

Robert N. Meroney*
David E. Neff#
Seong-Hee Shin+
Thomas C. Steidle+
Thomas Z. Tan#
Gang Wu+

Fluid Mechanics and Wind Engineering Program
Civil Engineering Department
College of Engineering
COLORADO STATE UNIVERSITY
Fort Collins, Colorado 80523

for

EXXON Research and Engineering Company
Florham Park, New Jersey 07932

on behalf of

An Industry Cooperative HF Mitigation Program
Vapor Barrier Subcommittee

July, 1988
(Revised February, 1989)

* Professor, Civil Engineering
# Research Associate
+ Graduate Research Assistant

CER88-89RNM-DEN-SHS-TS-TZT-GW-1

Colorado State University

PREFACE

INDUSTRY COOPERATIVE HF MITIGATION/ASSESSMENT PLAN

ANALYSIS OF VAPOR BARRIER EXPERIMENTS TO EVALUATE THEIR EFFECTIVENESS AS A MEANS TO MITIGATE HF CLOUD CONCENTRATIONS

This report is one of several work products generated by the Industry Cooperative HF Mitigation/Assessment Program. This ad hoc industry program was begun in late 1987 to study and test techniques for mitigating accidental releases of hydrogen fluoride (HF) and alkylation unit acid and to better estimate ambient impacts from such releases.

The hazards of HF have long been recognized, and operating practices have been aimed at minimizing the possibility of a release and mitigating the effects of a release should it occur. These practices have been continually monitored and improved to maximize safety protection based on the available technical data. This recent program has been aimed at further improvements based on new technical data.

This program has been sponsored and funded by twenty companies from the chemical and petroleum industries. These include Allied-Signal, Amoco, Ashland, Chevron, Conoco/Dupont, Dow, Elf Aquitaine, Exxon, Kerr-McGee, Marathon, Mobil, Phillips, Saras, Shell Internationale, Sohio, Sun, Tenneco, Texaco, Unocal, and 3M.

This document was prepared by the Fluid Mechanics and Wind Engineering Program, Colorado State University, as a part of its work for the Vapor Barrier Technical Subcommittee. The authors wish to acknowledge the interaction and encouragement of Rudolf Diener, EXXON Research and Engineering Company and Chairman of the Vapor Barrier Subcommittee, and the support and constructive criticism provided by all of the subcommittee members.

The results from this program are being published with the intent of making them available to any party with an interest in the subject matter. All are free to used these results subject to the rights of others. It is intended that the information presented herein will contribute to the further maximization of safety protection. However, neither the sponsors of this work nor their contractors accept any legal liability or responsibility whatsoever for the consequences of its use or misuse by anyone.

ABSTRACT

ANALYSIS OF VAPOR BARRIER EXPERIMENTS TO EVALUATE THEIR EFFECTIVENESS AS A MEANS TO MITIGATE HF CLOUD CONCENTRATIONS

Accidental releases of Hydrogen Fluoride (HF) can result in initially dense, highly reactive and corrosive gas clouds. These clouds will typically contain a mixture of gases, aerosols and droplets which can be transported significant distances before lower hazard levels of HF concentration are reached. Containment fences or vapor barriers have been proposed as a means to hold-up or delay cloud expansion, elevate the plume downwind of the barriers, and enhance cloud dilution.

Previous related field and laboratory experiments have been analyzed to estimate the effectiveness of barrier devices. The experiments were examined to determine their relevance to Hydrogen Fluoride spill scenarios. Wind tunnel and field data were compared where possible to validate the laboratory experiments. Barrier influence on peak concentrations, cloud arrival time, peak concentration arrival time, and cloud departure time were determined. These data were used to develop entrainment models to incorporate into integral and depth averaged numerical models. The models were then run to examine barrier performance for a typical Hydrogen Fluoride spill for a wide range of vapor barrier heights, spill sizes, meteorological conditions and release configurations. Finally the results of the data analysis and numerical sensitivity study were interpreted and expressed in a form useful to evaluate the efficacy of vapor barrier mitigation devices.

EXECUTIVE SUMMARY

ANALYSIS OF VAPOR BARRIER EXPERIMENTS TO EVALUATE THEIR EFFECTIVENESS AS A MEANS TO MITIGATE HF CLOUD CONCENTRATIONS

Accidental releases of Hydrogen Fluoride (HF) can result in initially dense gas clouds that will typically contain a mixture of gases, aerosols and droplets which can be transported significant distances before lower hazard levels of HF concentration are reached. Containment fences, vapor barriers, and water-spray curtains have been proposed as a means to hold-up or delay cloud expansion, elevate the plume downwind of the barriers, enhance cloud dilution, and/or remove HF from the gas cloud by deposition.

Exxon Research and Engineering Company, in conjunction with and on behalf of an ad hoc Industry Cooperative Hydrogen Fluoride (HF) Mitigation and Assessment Group has funded this study to assess the effectiveness of vapor barriers in diluting and delaying heavier-than-air HF vapor clouds. This data will provide a foundation of information to use to develop mitigation strategies, initialize numerical plume models, and/or design follow-up field and laboratory experiments. A secondary purpose of this study is to review evidence related to the accuracy and credibility of laboratory simulation of dense gas dispersion in the presence of vapor barriers. This information will be used to assess the value of future physical modeling experiments directed toward the mitigation of HF vapor clouds.

Previous related field and laboratory experiments have been analyzed to estimate the effectiveness of barrier devices. The experiments were examined to determine their relevance to Hydrogen Fluoride spill scenarios. Wind tunnel and field data were compared where possible to validate the laboratory experiments. Barrier influence on peak concentrations, cloud arrival time, peak concentration arrival time, and cloud departure time were determined. These data were used to develop entrainment models to incorporate into integral and depth averaged numerical models. The models were then run to examine barrier performance for a typical Hydrogen Fluoride spill for a wide range of vapor barrier heights, spill sizes, meteorological conditions and release configurations. Finally the results of the data analysis and numerical sensitivity study were interpreted and expressed in a form useful to evaluate the efficacy of vapor barrier mitigation devices.

Dilution Performance of Vapor Barriers in the Near-field Region

Eleven data sets from field and laboratory experiments dealing with the influence of vapor barrier fences and water spray curtains on the dispersion of dense gas clouds were examined. Tests were paired into sets of data which reflected the dilution of the cloud with and without the barriers present. Peak concentration ratios, cloud arrival time ratios, peak arrival time ratios, and departure time ratios were calculated for

each test pair. Consideration of the regions immediately downwind from the fences and sprays (distances less than 300 m downwind of the barriers) reveals that:

Vapor Barrier Fences:

@ Additional dilution occurs downwind of the fence as the turbulence produced by the shear at the top of the fence persists for about 30 fence heights. Near field reduction in concentrations ranges from 1.1 to 5.0.

@ Cloud arrival time, peak arrival time, and departure time ratios often increase directly downwind of a fence because lower winds in the wake advect the cloud more slowly. However, farther downwind the cloud arrives earlier because once the cloud leaves the wake region it is transported downwind with the greater depth averaged velocities associated with the increased cloud height. Near field increase in arrival, peak arrival, and departure times range from 1.1 to 5.0.

Water Spray Curtains: Removal Characteristics

@ Concentrations in a gas cloud will decrease abruptly as a result of chemical reaction and removal processes associated with HF and water spray interaction, even when accelerated entrainment associated with the water spray curtain is not considered. The removal efficiency will be a function of water/HF volume ratios, water droplet sizes and cloud concentrations.

Dilution Performance of Vapor Barriers in the Mid to Far-field Region

HF is hazardous at ppm levels. Thus, far-field concentrations are of interest in evaluating mitigation strategies. Most laboratory and field experiments were originally constructed to consider the behavior of flammable gases; hence, measurements were only taken at distances out to 1000 m downwind or less. Consideration of the regions modestly far downwind of barriers and spray curtains (300 m to 1000 m) reveals that:

Vapor Barrier Fences:

@ Entrainment levels return to pre-fence levels at distances greater than 30 to 50 fence heights downwind of the fence location. After that point the concentrations generally asymptote to levels found in the absence of the fence or barrier about 2000 m downwind of fences placed between 10 and 100 meters downwind of the spill site. A numerical model extrapolation suggests no discernible barrier effect will be present beyond 200 fence heights.

@ Peak concentrations measured during the experiments did not generally fall below 10,000 ppm of simulant or 150,000 ppm HF over the measurement domain.

Water Spray Curtains: Removal Characteristics

@ The reduction in HF cloud concentrations induced by water spray/cloud deposition processes persists at all downwind distances.

Proposed Entrainment Models

Given a box or depth-integrated type numerical model simple expressions to account for the increased entrainment associated with water spray curtains or fence barriers may be used with confidence. These models do not account for chemical reactions, deposition, gravity current reflection, rapid flow speed up through a porous barrier, or the presence of a hydraulic jump downwind of a barrier. Both the initial dilution and post-barrier concentration decay are predicted well.

Laboratory Simulation of a Hydrogen Fluoride Spill

The capabilities and limitations of physical modeling techniques for HF gas clouds were reviewed. Performance envelopes were constructed to illustrate the constraints of facility size and gravity spreading. The following conclusions were made:

@ Laboratory simulation of a pure HF release with an isothermal simulant is not recommended. Reliable simulations would be limited to prototype wind speeds greater than 5 m/sec at scales less than 1:100. Model concentrations must be adjusted upward by a factor of 15 in the far downwind regions.

@ Laboratory simulation of a pre-diluted HF cloud can be accomplished. Reliable simulations should be possible at all distances for prototype wind speeds greater than 5 m/sec at scales less than 1:100.

TABLE OF CONTENTS

LIST OF TABLES

LIST OF FIGURES

LIST OF SYMBOLS

Symbol	Definition	Units
A,a,b, c,d,e	Regression constants in ANOVA	--
A_i	Area of intersection between gas cloud and water spray	$[L^2]$
B	Characteristic cloud width calculated by cross-section averaged numerical programs	[L]
C_m	Model concentration	--
C_p	Prototype concentration	--
C_w, C_{wi}, C_{wf}	Concentrations measured with barrier present	--
C_{wo} C_{wof}	Concentrations measured without barrier present	--
C_D	Fence drag coefficient factor	--
C_p^*	Molar specific heat capacity at constant constant pressure	$[L^2/T^2]$
D	Molecular diffusivity	$[L^2/T]$
d_g	Diameter of water spray intercept area with gas clouds	[L]
f-N	Surface pattern comparison factor, % predicted within N	--
Fr	Froude number, $U^2/(g(SG - 1)L)$	--
$\underline{Fr}$	Flux Froude number, $U^3L/(Qg(SG - 1))$	--
g	Gravitational acceleration	$[L/T^2]$
H_f	Fence height	[L]
$H_{V.G.}$	Vortex generator height	[L]
H	Characteristic cloud height calculated by cross-section averaged numerical programs	[L]
L_c	Characteristic length, typically 10 m	[L]

Symbol	Definition	Units
L_{ci}	Characteristic length for instantaneous spills used by Koenig and Schatzman (1986)	[L]
L_{cc}	Characteristic length for continuous spills spills used by Koenig and Schatzman (1986)	[L]
L_s	Lateral water-spray nozzle separation	[L]
M,MW	Molecular weight	--
MR	Multiplicative factor used in water-spray entrainment model	--
ν	Kinematic viscosity	$[L^2/T]$
N	Number of water-spray nozzles	--
P	Fence porosity	--
Pe	Peclet number, UL_c/D	--
π	3.1417	--
Q,Q_s	Source strength spill rate	$[L^3/T]$
Q_e	Air entrainment rate	$[L^3/T]$
Q_G	Spill rate gas	$[L^3/T]$
Q_L	Spill rate liquid	$[L^3/T]$
Ri	Richardson number, $g(1 - SG)L_c/U^2$	--
ρ	Density	$[M/L^3]$
RH	Relative humidity	--
S	Water-spray intersection interval	[L]
SG	Specific gravity	--
T_{amb}	Ambient air temperature	[θ]
T_{dap}	Dew point temperature	[θ]
T_s,T_f	Source gas temperature	[θ]
Ta_w,Ta_{wo}	Cloud arrival times with and without barrier	[T]

Symbol	Definition	Units
Tpa_w, Tpa_{wo}	Peak concentration arrival time with and without barrier	[T]
Tda_w, Tda_{wo}	Cloud departure times with and without barrier	[T]
U_{ci}	Characteristic wind speed for instantaneous spills used by Koenig and Schatzman (1986)	[L/T]
U_{cc}	Characteristic wind speed for continuous spills used by Koenig and Schatzman (1986)	[L/T]
U_{10}	Wind speed at 10 m reference height	[L/T]
U(H)	Wind speed at fence height	[L/T]
U_g	Frontal velocity of dense cloud	[L/T]
u_*	Friction velocity	[L/T]
V,Vol	Total gas volume released	$[L^3]$
$\underline{V}_c$	Dimensionless continuous volumetric spill rate, $Q/(UL^3)$	--
V_i	Dimensionless instantaneous volume spill, Vol/L^3	--
w_e	Air entrainment rate	[L/T]
w_*	Convection velocity	[L/T]
x,y,z	Coordinate system, origin at spill location	[L]
x_f	Downwind distance from spill location to fence	[L]
Y	Downwind distance used for Thorney Island Trials	[L]
Z_o	Surface roughness length	[L]

DEFINITION OF KEY TERMS AND ABBREVIATIONS

Arrival Time		The time after the release a minimal level of concentration arrives at a specified downwind location
Peak Arrival Time	-	The time after the release a peak concentration arrives at a specified downwind location
Departure Time	-	The time after the release the concentration falls below a minimal level at a specified downwind location
Arrival Time Ratio	-	The ratio of the cloud arrival time with a barrier to the cloud arrival time without a barrier at a specified downwind location
Peak Arrival Ratio	-	The ratio of the cloud peak arrival time with a barrier to the cloud peak arrival time without a barrier at a specified downwind location
Departure Time Ratio	-	The ratio of the cloud departure time with a barrier to the cloud departure time without a barrier at a specified downwind location
Concentration Ratio	-	The ratio of the peak concentration with a barrier to the peak concentration without a barrier at a specified downwind location

ANALYSIS OF VAPOR BARRIER EXPERIMENTS TO EVALUATE THEIR EFFECTIVENESS AS A MEANS TO MITIGATE HF CLOUD CONCENTRATIONS

1..0 INTRODUCTION

Over the past twenty years there has been a marked increase in concern about the consequences of large and small scale releases of flammable or toxic gases into the atmosphere. This new awareness reflects the increasing scale, in number and extent, of industrial and transport operations involving these hazardous materials. The occurrence of recent disastrous accidents has focused attention on the potential risks of these operations. Regulation of production, storage and transport of such products, the design of mitigation equipment, and the preparation of accident response strategies requires an accurate evaluation procedure to predict the consequences of hazardous gas release.

Exxon Research and Engineering Company, in conjunction with and on behalf of an ad hoc Industry Cooperative Hydrogen Fluoride (HF) Mitigation and Assessment Group has funded this study to assess the effectiveness of vapor barriers in diluting and delaying heavier-than-air HF vapor clouds. This data will provide a foundation of information to use to develop mitigation strategies, initialize numerical plume models, and/or design follow-up field and laboratory experiments. A secondary purpose of this study is to review evidence related to the accuracy and credibility of laboratory simulation of dense gas dispersion in the presence of vapor barriers. This information will be used to assess the value of future physical modeling experiments directed toward the mitigation of HF vapor clouds.

Examination of the Acute Hazardous Events Database prepared by EPA (and earlier statistics about vapor cloud accidents) reveals that three-quarters of all events occur in-plant (production, operations or storage) and one-quarter occur in-transit (truck, rail, pipeline, etc.). In-plant events are about equally divided between storage, valves and pipes, and processing. In-transit events are associated with truck and rail modes. Collisions and leaks cause most transportation deaths and injuries Storage and pipeline failures cause the majority of in-plant deaths and injuries (Crum, 1986; Wiekema, 1984; Davenport, 1977).

Thus, the majority of hazardous gas accidents result from failure of confinement whether from a stationary tank, pipeline or mobile storage container. Disregarding whether the loss of containment is due to a small leak, a complete rupture, or continuous high volume release from an aperture, the puff, plume or cloud will interact with the container, the nearby buildings, vapor barriers, water spray or the ground and the surface boundary layer to produce dilution behavior which can not be predicted by conventional isolated plume theories.

It is appropriate to review what is known about the physics of the initial formation phase of a cloud or plume, the interaction of dense gas clouds with barriers and the ability of fluid modeling to illuminate the entrainment mechanisms further.

1.1 The Formation Phase of a Hazardous Cloud

Hartwig and Flothman (1980) prepared diagrams outlining important processes occurring during a hazardous gas release scenario. They identified self-generated dilution as an important unresolved issue during consequence analysis. Brenchley (1981) and DeSteese (1982) reviewed the hazard characteristics of operation, storage and transportation for ammonia and liquid petroleum gas products. They tabulated the typical container sizes, accident statistics, and hazards. They recommended research on mixing models, source physics, and the instantaneous character of the cloud concentration distribution. McQuaid (1982) identified three phases in the estimation of the consequences of a hazardous cloud release:

a.) The initial formation of a cloud or plume near the source,
b.) The dispersion of the cloud or plume to where it ceases to be a hazard, and
c.) The consequences if the cloud or plume is ignited or passes over a population.

The formation phase of cloud generation is dependent on the quantity of gas released (or rate of evolution from a liquid), the nature of the release (leak or rupture), and the geometry of tank, pipe and/or local buildings. Griffiths and Kaiser (1979) examined in detail the implications of different types of spills of ammonia. They evaluated small and large releases from vapor spaces in pressurized containers, small and large releases from liquid spaces, onto land, onto and under water and the effect of buildings. For ammonia they determined small leaks from vapor spaces were not a major problem, but they concluded further research was necessary about:

a.) The effect of intermediate size holes from vapor spaces in storage containers,
b.) The interaction of plumes with nearby buildings which could destroy plume buoyancy or alternatively encourage dense plume persistence, and
c.) Plume release configurations which might suppress lift-off.

Other relevant studies have examined the character of sources resulting from the evaporation from liquid pools (Shaw and Briscoe, 1978), mixing down wind of relief valves (Jagger and Edmondson, 1981; Samimy and Addy, 1983), cloud formation during massive containment rupture or explosion (Kaiser and Walker, 1978; Jagger and Kaiser, 1980; Bodurtha, 1980), and plume formation during losses from large exhaust jets (Abramovich, 1963; Ricou and Spalding, 1961; Wilson, 1981). Most quantitative estimates are based on conjecture about the release process, most verification is based on examining plume behavior downwind from the

source, and few measurements are available in the direct vicinity of the release.

Hardee and Lee (1975) developed a simple model to predict the growth of a hazardous cloud near a rupture-type containment accident. The model used two-phase flow expansion in an isentropic process. Total momentum is calculated and used to predict subsequent cloud growth, but no adjustments are made for the possible consequences of plume buoyancy or interaction with surrounding structures. Hirst (1986) has shown that liquid mass release through short circular orifices in pressurized propane tests are reliably predicted by the Bernoulli equation, but for gas or two-phase situations the mass flow is substantially less. At the other extreme of sophistication Wilson (1981) has developed a jet-plume model for estimating dispersion downwind of a buried pipeline. He incorporated transient mass release rates, expansion and acceleration of the compressible plume outside the rupture area, interaction of the supersonic jet with soil crater walls, and entrainment of ambient air into the head of the starting plume. This excellent model was calibrated and compared against full scale pipe-rupture experiments performed in Alberta during 1978. Validation of all possible source conditions against full-scale field tests is possible, but represents a very costly approach to model verification. Fluid modeling should provide equivalent data at great savings.

1.2 Fluid Modeling of Atmospheric Phenomena

Recently Briggs and Binkowski (1986) reviewed the state of numerical model prediction of plume behavior in the atmosphere. They concluded *"a major need is for diffusion experiments, both in the field and in laboratory settings. The laboratory studies are needed to test theoretical results in specific simplified situations that are free of confounding influences."* The acceptance of fluid modeling by the meteorological community as a viable prediction tool is reaffirmed through their assertion that *"confidence in these tools [fluid modeling] has increased to the point that they have been used extensively to investigate diffusion from releases on and near buildings and terrain features. ....In addition to being less expensive than field experiments, laboratory modeling offers control over the meteorological variables, so that both the flow and surface characteristics can be idealized....It is obvious that this tool has not been fully exploited...it makes sense to use laboratory facilities as much as possible."*

Complex Terrain and Building Aerodynamics:

Successful modeling of some of the more complex atmospheric surface layer and building aerodynamic phenomena in a wind tunnel have only been accomplished in the last fifteen years. Although guidelines for modeling flow over complex terrain are essentially similar to those for modeling hydraulic flows or flow around buildings, a few unique features are different. Irregular terrain may alter atmospheric airflow characteristics in a number of different ways. These effects can generally be grouped into those due to inertial-viscous interactions

associated with a thick neutrally stratified shear layer and to thermally induced interactions associated with stratification or surface heating (Meroney, 1980).

Meroney (1980) compared three model/field investigations of flow over complex terrain, suggested performance envelopes for realizable modeling in complex terrain, and discussed recent laboratory studies which provide data for valley drainage flow situations. Not all of the model/field comparison experiments performed in the past were successful. Many early studies had model approach flow velocity exponents near zero, were modeled as neutral flows when the field observed strong stratification effects, or simulated unrealistic boundary layer depths, integral scales, or turbulence intensities which did not match their atmospheric counterpart. But few studies claimed unreasonable correlation, and some were strongly self-critical. Nonetheless most studies accomplished their prestated limited objectives. It would appear that the simulation wisdom developed in the last few years is appropriate for physical modeling of flow over complex terrain.

The interaction of an approach wind field with bluff bodies or structures constructed on the earth's surface is broadly termed "Building Aerodynamics." In a review article on this subject Meroney (1982) discusses the character of bluff body flow about rectangular buildings and cylindrical cooling towers. Defects in velocity profiles can easily persist to 10 to 15 building heights downwind. Turbulence excesses and deviations in temperature profiles may persist to 20 or 30 building heights downwind. Field and laboratory measurements of plume dispersion about the Rancho Seco Nuclear Power Station in Sacramento, California, confirm that cooling tower wake effects persist for significant downwind distances under a variety of stratification conditions (Allwine, Meroney and Peterka, 1979; Kothari, Meroney and Bouwmeester, 1979).

For accidental releases the quantity desired for safety measures is the "immission," which is either the concentration of the gas or the dosage. Such quantities depend upon the "emission," which is the released quantity of mass or volume, and the "transmission," which is the combined effect of the wind field at the moment of release and thereafter plus the mixing properties of the wind field determined by obstacles, surface roughness, and thermal heating. The transmission function can be divided into three regions--the region-of-release, the near-field, and the far-field. The region-of-release depends upon the source characteristics and its immediate surrounding. The near-field region is governed by the local characteristics of the industrial plant and its surroundings. In the far-field the ground is characterized by homogeneous surface roughness and heating characteristics. These regions will depend upon the nature of the mitigation device or barrier considered; for example a fence may be expected to perturb the velocity field for 10 heights downwind, the turbulence field for 20 to 30 heights downwind, and the entrainment rate over a similar distance. On the other hand, a water spray curtain produces most of its dilution or reduction very close to the water spray device. The far-field region will exist once dense-gas gravitational effects are minimal and the perturbations of barriers decay. The effect

of water-spray removal of vapor or particles will, of course, persist at all downwind distances, to the extent that it does not modify (reduce) the dynamic mixing of the vapor cloud. The distance to such a region will depend upon both spill size and barrier height.

A number of studies have been performed in the CSU Fluid Dynamics and Diffusion Laboratory to establish the near-field effect of buildings on flow fields and dispersion. Hatcher et al. (1977) examined flow and dispersion in stratified flow downwind of the Experimental Organic Cooled Reactor, Idaho Falls; Allwine et al. (1979) studied the Rancho Seco Reactor, Sacramento; Kothari et al. (1979) studied the Duane Arnold Energy Center, Iowa. In each case field measurements were compared to laboratory measurements with good agreement.

Relatively few studies have examined the composite effect of combined building and industrial equipment upon plume dispersion. Recently Plate and Baechlin (1987) reported a wind tunnel study of dispersion over a model of one of the largest chemical plants in the world, the Badische Anilin und Soda Fabrik (BASF) in Ludwigshafen, FRG. Measurements of wind field and concentration over the 1:500 scale model are being used to develop a catalog of ground level concentration fields for typical plant situations. Point sources of neutral density source gases were studied to produce generic plume behavior for different wind directions.

Hazardous Gas Dispersion:

Meroney (1982) reviewed the use of fluid modeling to evaluate the dispersion of dense gases. He notes that wind tunnels have simulated a wide range of conditions associated with dense gas transport and dispersion (bunded tanks, spills on water, water spray mitigation equipment, vertical emission through stacks, etc.) Measurements of dense fluid behavior in both air and water facilities appear reproducible and consistent. Idealized release configurations appear optimal for testing numerical or analytical models. Wind tunnels are primarily limited by operational constraint associated with the necessary low wind speeds and low Reynolds numbers.

In a two volume Gas Research Institute report Meroney (1986) provides guidelines for using fluid modeling to generate Liquid Natural Gas (LNG) dispersion information. The second volume reviews the fluid modeling science and the extensive model/field validation efforts performed over the last ten years. The wind tunnel was found to reproduce field data over a wide variety of scales. The comparisons between field and model data from the Thorney Island Freon-air experiments, the Maplin Sands LPG and LNG experiments, and the China Lake LNG experiments were particularly satisfying.

More recently British Maritime Technology (Davies and Inman, 1986) has completed a report on their own fluid model experiments performed to reproduce the Thorney Island experiments, and, again, plume shape and

concentration fields were reproduced in almost every respect including instantaneous structure of the cloud interior. They concluded that,

a.) There was no evidence that the neutrally stable wind tunnel boundary layer failed to represent the dispersion in the more stable full-scale atmospheric conditions,

b.) Reductions in the downwind dispersion distance to a given concentration level due to vapor fences were reproduced by the laboratory experiments, and

c.) For trials involving sharp-edged mixing elements, such as buildings or fences, there was no evidence for a lower validity level for the simulation Reynolds number. For continuous and instantaneous releases onto unconfined terrain the lower limits of the simulation Reynolds number ($U_{10m}*L_{Dm}/\nu$) for conservative simulations (ie. model/full scale > 1) were 100 and 30000 respectively. (U_{10m} is the scaled 10 m velocity in the wind tunnel, and L_{Dm} is the buoyancy length scale of the release).

Releases of pressurized, superheated Hydrogen Fluoride are known to produce a heavy (Specific Gravity = 10), cold, two phase vapor plume close to the source. (Vapor or boiling pool releases of HF will not produce such dense clouds.) The gas cloud subsequently condenses water vapor, changes molecular polymer state through dissociation and association and consequently absorbs and releases heat to the surroundings. Special problems associated with the simulation of Hydrogen Fluoride spills and the subsequent behavior of its vapor cloud are discussed further in Section 7.0 of this report.

Dense Vapor Interaction with Fences, Barriers and Obstacles

Dense gas plumes dispersing over the ground undergo mixing due to the turbulence produced by gravity driven vapor spreading and the turbulence associated with the atmospheric surface flow. However, these conditions may be considerably perturbed by the additional complications of surface obstructions. Such interference may cause additional plume dilution or temporary pooling of higher gas concentrations. Researchers at Colorado State University have examined a cross section of barrier, water spray and obstacle configurations. Tests include the influence of high and low barrier dikes (Meroney et al., 1976, 1977, 1980, and 1981); tanks, fences and vegetation barriers (Kothari and Meroney, 1981); and fences and vortex generators (Kothari and Meroney, 1982), and water spray curtains (Andriev et al, 1983, Heskestad et al, 1983, Meroney and Neff, 1983, and Meroney et al, 1983). Recently, Neff and Meroney (1986) completed a pre-field-test wind tunnel series of the Falcon LNG vapor barrier test series, and are now preparing a post-field test program on the Falcon tests.

British Maritime Technology (Davies and Inman, 1986), as mentioned above, completed a series of wind tunnel simulation tests of some of the

Thorney Island dense gas spill experiments which included barriers. These tests were found to replicate most features of the field experiments, and they did not seem to be sensitive to model perturbations associated with low Reynolds numbers or low Peclet to Richardson number ratios developed during the model tests.

Researchers at the University of Hamburg (Konig and Schatzmann, 1986) examined the behavior of instantaneous and continuous releases of dense gases in a wind tunnel when dispersing in the vicinity of model walls, between model buildings, over model street canyons, and when confined by fences. Their data is unique in that they studied situations which actually tend to "reduce" dilution rather than enhance it. Significantly, the release scenarios they considered are frequently encountered in industrial complexes and cities.

1.3 Report Organization

The previous remarks summarize the current status of understanding for dense gas dispersion, obstacle (buildings, tanks, dikes, fences and sprays) and terrain aerodynamics and physical simulation of these flows. Currently there are no analytic algorithms or numerical programs capable of producing the necessary flow defect/dispersion information. The following chapters discuss additional insight gathered during the detailed analysis of the dense gas dispersion literature. Chapter 2.0 considers specific characteristics of Hydrogen Fluoride gas and proposes simple algorithms to allow for additional entrainment of air or removal of HF developed by vapor barriers or water spray curtains. Chapter 3.0 summarizes the applicable data bases available during this review. Chapter 4.0 provides the results from further evaluation of the data bases identified in Chapter 4.0. In Chapter 5.0 the entrainment models proposed in Chapter 2.0 are compared to the data extracted from previous studies in Chapter 3.0. Subsequently, the calibrated numerical models are used to predict potential mitigation of HF spills by sprays and barriers in Chapter 6.0. Chapter 7.0 summarizes some thoughts about the effective simulation of HF cloud behavior through fluid modeling. Conclusions drawn from the review, analysis, and numerical interpretations are provided in Chapter 8.0.

2.0 DISPERSION OF HYDROGEN FLUORIDE GAS CLOUDS

Hydrogen fluoride is a colorless, corrosive toxic liquid or gas, depending on the temperature. Hydrogen fluoride is used to prepare fluorides, to manufacture fluorine, as a catalyst in isomerization, condensation, dehydration, polymerization, and hydrolysis reactions, and a fluorinating agent in organic and inorganic reactions. It is also used as an alkylation catalyst in the petroleum industry, for etching and polishing of glass, and in the manufacture of aluminum fluoride and synthetic cryolite.

Because hydrogen fluoride's boiling point of 292.67°K (19.5°C) is often exceeded by the temperature at which it is transported or used, it is typically shipped in cylinders under its own vapor pressure of 2.1 kPa (0.3 psig) at 20°C. The gas is both toxic and corrosive. The concentration that produces acute effects varies with the time of exposure. The American Industrial Hygiene Association recommends levels of EPRG1 = 5 ppm, EPRG2 = 20 ppm and EPRG3 = 50 ppm for the Emergency Response Planning Guidelines. These are exposure levels that the general populace can experience without receiving other than mild transient adverse health effects, irreversible or serious health effects, or developing life-threatening health effects, respectively. Less severe exposures cause irritation of the nose and eyes, smarting of the skin, some degree of conjunctival and respiratory irritation. The 1979 ACGIH has also established a Threshold Limit Value (TLV) of 3 ppm (2 mg/m^3) for exposures of people in occupational settings.

2.1 Source Characteristics

Diener (1988) suggested two typical scenarios for hypothetical HF releases. One covers HF Alkylation units and the other covers typical transport and production scenarios. For conservatism, the upper bounds on release rates were deliberately set on the high side. The envelopes indicated are however fairly typical and representative.

HF Alkylation Unit Scenarios

Pressure	:	100 - 200 psig
Temperature	:	100°F (57°C)
Flowrate	:	1 - 500 gpm HF or alkylation unit acid
Duration	:	1 - 10 minutes
Release Type	:	release in middle of typical refinery setting from line rupture (1" - 3" range), flange leak, pump mechanical seal leak, etc; majority of releases at or near grade but possibility of elevated releases
Aerosols		total aerosolization expected (i.e. no liquid pool)

Transportation/Production Scenarios

Pressure	:	10 - 80 psig
Temperature	:	40 - 100°F (4 - 57°C)
Flowrate	:	1 - 100 gpm pure anhydrous HF
Duration	:	1 - 10 minutes
Release Type	:	release in middle of typical chemical plant/tank farm setting or from tank truck/rail car during transit resulting from line rupture (1" - 3" range), flange leak, pump mechanical seal leak, etc.; majority of releases at or near grade but possibility of elevated releases as well as all-vapor releases
Aerosols	:	liquid pool formation possible, especially at low pressure/temperature range

2.2. State Equations for Hydrogen Fluoride

HF can exist as unassociated HF or as an HF polymer, with association (an exothermic process) favored by low temperatures. When pressurized superheated HF is released into the atmosphere, a series of competing phenomena occur. As the turbulent jet expands and entrains air, any liquid droplets entrained by the flashed HF vapor will vaporize thereby drastically reducing the cloud temperature. Air dilution will reduce the HF partial pressure thus favoring dissociation but the temperature reduction resulting from liquid HF vaporization will favor HF association.

Simultaneously, the rapid temperature drop due to entrained liquid HF vaporization will condense out moisture from the ambient air as frost or droplets. This condensed water will react with the HF forming a stable, maximum boiling water/HF azeotrope. The result is a persistent HF/water fog. The process of condensing water from the ambient is exothermic, as is the process of mixing HF and water in the liquid phase. The net result is a cloud whose properties are changing significantly as it entrains air and is advected downwind.

Schotte published a paper in 1987 that discussed measurements of vapor HF/air mixtures with relative humidities from 0% to 100%. He developed equations for liquid HF releases to predict temperature changes, onset or disappearance of fog, amount of fog, fog density, and concentration of HF in the fog. EXXON Research and Engineering incorporated Schotte's model along with a flash algorithm into a FORTRAN program (Diener, 1988b). Allied Corporation produced graphs of the HF-H_2O-Air system from the Schotte equations coded by EXXON (Hague, 1988). Calculations for HF release conditions (pressurized superheated HF) suggest that the initial source cloud consists of 80% - 90% liquid aerosol and initial cloud temperatures of 0 to 14°C. The subsequent rise and fall or liquid aerosol fraction and cloud temperature are quite complex, but the effective cloud density decreases monotonically with increase in entrained air (See Figures 2.1-1 and 2.1-2). It is this cloud density

state relation which determines cloud spreading behavior and effects the turbulent mixing rates.

Any gas or hypothetical gas which reproduces this density state behavior with dilution can be used in laboratory or numerical models to predict cloud transport and dilution. An ideal gas can be conceived with molecular weight of 20 (same as HF), a very cold source temperature, and a specified molar specific heat capacity that will have the same number of molecules per volume as an HF aerosol cloud. Careful selection of the ideal gas molar specific heat capacity permits the ideal gas to reproduce the density behaviors noted in Figures 2.2-1 and 2.2-2. Figures 2.2-3 through 2.2-7 examine the combinations of temperature and molar specific heat capacity required to reproduce the Schotte density curves. Figures 2.2-3, 2.2-4, and 2.2-5 examine density versus lbs. Air/lbs. HF released ratio. Figure 2.2-6 indicates the variation of cloud density with mole fraction of HF, and Figure 2.1-7 displays the consequent diluted cloud temperatures. Note that ridiculously low ideal gas temperatures (circa 5 - 20°K) are required to represent in a gas the number of gas molecules stored by the real cloud in a liquid aerosol.

Also noted on Figures 2.2-3 to 2.2-5 are the molecular weight values (205 - 1037) required for an isothermal gaseous simulant to reproduce the extremely large initial cloud specific gravity (S.G. = 12 to 20) and subsequent density history. Note that an isothermal simulant will not permit a buoyant cloud to exist at low concentrations. Since the densest isothermal cloud simulant commonly used in laboratory measurements is SF_6 (S.G. = 5.05), it is not likely that laboratory simulations will correctly consider the inertial characteristics of a dispersing HF cloud modeled as a pure HF release. This will be discussed further in Chapter 7.0, where laboratory modeling of pre-diluted HF plumes is found acceptable.

2.3. Hydrogen Fluoride Spill Experience

Although accidental releases of Hydrogen Fluoride have occurred , little information can be gleaned from post spill analysis about the cloud mixing process. Hence, in 1986 Amoco Oil Company and the Lawrence Livermore National Laboratory (LLNL) conducted a series of six experiments involving atmospheric releases of anhydrous hydrofluoric acid at the Department of Energy Liquefied Gaseous Fuels Test Facility. The purpose of these tests was to examine source characteristics, dispersal properties and water spray mitigation techniques. A description of the experimental design and limited results were presented in papers by Blewitt et al. (1987a, 1987b).

These tests were designated the "Goldfish" test series by LLNL. Test conditions extracted from the Blewitt et al. (1988a) paper are shown in Table 2.3-1. Note that the first three tests were unmitigated releases (i.e. no water sprays); whereas the next three tests considered the mitigating influence of water sprays. The first three tests (Goldfish Trials 1, 2, and 3) have been used in Chapter 5.1 of this report to validate the numerical models used herein for entrainment model evaluation. Goldfish Trial 1 was also chosen to be the reference case

against which sensitivity calculations discussed in Chapter 6.0 were performed for the mitigating effects of water sprays and vapor fences operating at various locations, wind speeds, spray strengths and barrier heights.

During small scale tests Allied Corporation observed that up to 78.8% of the HF could be removed from a gas cloud by water sprays when water/HF volume ratios were 64/1. Blewitt et al. (1988b) reported reductions of approximately 36% to 49% in downwind concentrations during Goldfish Trials 5 and 6. This report did not examine any other data which included extraction of gases from the cloud by mitigating devices, but both the reduction and diluting aspects of water sprays have been considered.

The kinematics and dynamics of the initial motion of a HF cloud will be determined by the ratio of gravity forces acting on the cloud and the inertia of the ambient atmosphere together with the ratio of the source strength of the HF cloud and the diluting capacity of the atmosphere. The appropriate governing parameters for an instantaneous HF cloud release will be the Froude number, $Fr = U^2/(g(SG-1)L)$, and the Volume Ratio, $V_i = V/L^3$, where U is a characteristic wind speed, L is a characteristic length scale, and SG is the cloud specific gravity at release conditions. For a continuous HF plume the relevant parameters are the Flux Froude number, $\underline{Fr} = U^3L/(Qg(SG-1))$ and the Volume Flux Ratio, $\underline{V_o} = Q/(UL^2)$, where Q is the source volume flow rate at release conditions. Based on the scenarios described by Diener (1988) in section 2.1 above the parameter ranges relevant for typical HF spills of pure HF are:

Instantaneous Spills

$Fr = 0.0011$ to 0.11,

$V_i = 0.15$ to 1.5,

Continuous Spills

$\underline{Fr} = 0.045$ to $22{,}600$, and

$\underline{V_o} = 0.000005$ to 0.025.

An alternative range of spill conditions can be identified if one focuses attention on the behavior of the HF plume only after all unflashed HF evaporate (i.e. at minimum cloud temperature). This condition typically occurs once the mass ratio lbm air/lbm HF is greater than 5. At this state point the cloud volume is larger, but the cloud specific gravity is significantly less. For many situations only jet mixing occurs below a mass fraction ratio of 5; hence, gravity mixing dynamics are not dominant in this region. Based on the scenarios described by Diener (1988) in section 2.1 above the parameter ranges relevant for typical HF spills of pre-diluted HF are:

Instantaneous Spills

Fr = 0.035 to 3.5,

V_i = 1.2 to 12,

Continuous Spills

Fr = 0.171 to 85,500, and

V_c = 0.00004 to 0.2.

These parameter ranges are outlined on Figures 2.3-1 and 2.3-2. The figures also contain points reflecting the conditions for which various dense gas experiments relevant to HF dispersion were obtained. Notice there are wide parameter ranges where no data has been taken; thus, conclusions drawn from tests performed over the limited space of the spill envelope must be extended with great caution to other spill conditions.

2.4 Entrainment Models for Vapor Barriers and Water Spray Curtains

Models for dense-cloud dispersion are desired which produce the detailed nuances of behavior perceived during laboratory and field experiments. When a flow field is only weakly three dimensional so that some dimensions can be decoupled from the others, a set of simple relations can be obtained by integrating the conservation equations over that dimension. When the flow situation is steady and diffusion in one direction is weak with respect to advection, it is possible to integrate over a plume cross-section and calculate plume width, average height, and cross-section averaged velocities, concentrations, temperatures, and humidity. Such a "box" type model is numerically very fast since the conservation equations reduce to a set of coupled ordinary differential equations. Alternatively when vapor generation is transient, and there are opportunities for upwind flow, a set of coupled partial differential equations of only two dimensions and time can be created by integrating the conservation equations over just the depth. Such a "shallow layer" or "slab" type model provides information about time- and space-dependent cloud widths, heights, and depth-averaged velocities, concentrations, temperatures, and humidities.

Such models can be modified to handle the increased dilution which occurs in the presence of water spray curtains or vapor barrier fences. A box model (Meroney and Lohmeyer, 1984; Meroney, 1983; and Andreiev et al., 1983) and a slab model (Meroney and Lohmeyer, 1984, and Meroney, 1984a and 1984b) have been adapted to consider HF dilution by water sprays and vapor barrier fences.

Both numerical models normally use the concept of an entrainment velocity, we, across the upper cloud surface to mix the cloud with ambient air. The entrainment velocity is a semi-empirical function of boundary-layer and cloud variables such that,

$$w_e = f(U_g, u_*, w_*, Ri_*),$$

where U_g = plume frontal velocity,
u_* = friction velocity,
w_* = convective velocity, and
Ri_* = local plume Richardson number.

Various expressions which describe the entrainment of air into dense gas clouds have been proposed for isolated clouds dispersing in homogeneous surroundings (Blackmore et al., 1982; Ermak et al., 1982; Havens and Spicer, 1985; Meroney, 1984a).

Removal of HF from Gas Cloud by Water Sprays

Reductions in HF cloud concentrations can occur through chemical reaction between the cloud and water spray. HF reacts with the liquid water and leaves the cloud as the water deposits on the ground. Laboratory and field tests described by Blewitt et al. (1987c) measured HF removal ranging from 9 to 80%.

The chemical mechanisms, their rate constants, and the manner in which the cloud reacts with different size droplets has not been documented. A simple removal rate model can be presumed, however, that can be used to project cloud behavior after a portion of the HF mass is removed. Care must be taken to assure corrections are applied to the cloud fluxes of momentum, mass, and energy after removal.

Entrainment due to a Vapor Barrier

A vapor barrier or fence placed downwind of a dense vapor cloud can induce a variety of fluid mechanic responses by the cloud. Britter (1982) reviewed a number of special hydraulic effects expected from stratified fluids in the presence of surface obstacles or sloping terrain. Later Rottman et al. (1985) considered the Thorney Island Phase II trials with respect to the observed gravity current behavior. Essentially the cloud may behave like a moving layer of liquid traveling either as a rapid (super critical) or tranquil (subcrictical) flow, where $Fr > 1$ or $Fr < 1$, respectively passing over a surface obstruction. When the flow is rapid the obstacle may block and reflect the cloud upwind; increase upwind depth and accelerate the cloud over the obstacle; or increase upwind depth, accelerate the cloud over the obstacle, and then mix aggressively in a hydraulic jump. Calculations suggested that with low ambient winds the gas cloud would not pass over a fence if the height of the fence is more than 2.5 times the height of the approaching gravity current. When the approach flow is tranquil and the cloud height is greater than the fence height, then the cloud upper surface may dip down briefly as it passes over the obstacle.

Rottman et al. also concluded that when a rapid flow passes through a porous fence the cloud may accelerate and the cloud height will decrease. This could lead to earlier arrival times downwind of the fence.

If a barrier interacts with a cloud after the gravity driven phase of its motion is reduced, then the primary action of the fence will be to modify local wind profiles and increase turbulence due to strong wind shears located at the top of the fence. This increased turbulence will increase air entrainment into the cloud. Since the turbulence will decay more or less linearly out to about thirty fence heights downwind, the dense cloud will perceive an initial step increase in mixing rate which then decays slowly back to ambient levels. The entrainment rate due to a barrier may be expected to be proportional to the approach wind speed at fence height, U(H), a fence drag coefficient, C_D, and fence porosity, P. The following simple model is proposed to described the increased entrainment resulting from a vapor barrier fence:

$$(w_e)_{fence} = C_D U(H)(1 - P)(1 - (x - x_f)/(30H)),$$

where x is distance downwind of the source, x_f is fence location, and the relation is not used downwind of x_f. This model will be used in the numerical models to compare with selected field and model data. Subsequently, it will be used to prepare sensitivity calculations of reference case Goldfish Trial No. 1 in the presence of vapor barriers.

Table 2.3-1 Spill and Meteorological Conditions During Goldfish Trials

Goldfish Spill Conditions:
1986 Amoco, LLNL Tests
RNM - 22 June 1988

Property	Number 1	Number 2	Number 3	Number 4	Number 5	Number 6
Spill Conditions						
Spill Rate (gpm)	469.2	175.1	171.6	67.5	32.5	33.0
HF Temp (oC)	40.0	38.0	39.0	36.0	40.0	38.0
Duration (sec)	125.0	360.0	360.0	840.0	960.0	960.0
Wind Speed (m/s)	5.6	4.2	5.4	6.8	3.8	5.4
Air Temp (oC)	37.0	36.0	26.5	21.3	21.3	21.5
Dew Point (oC)	-8.5	1.1	6.6	-2.0	5.6	4.6
RH %	5.0	12.0	28.0	20.0	35.0	32.0
Spray Conditions						
X-spray (m)				14.3	30.5	31.7
Spray width (m)				8.5	22.9	22.9
Number Nozzles				4.0	25.0	25.0
Height nozzles (m)				3.7	0.3	3.7
Q water (gpm)				67.5	700.0	700.0
time on (min)				0-7	0-9	9-?
time off (min)				7-14	9-17	0-9
Numerical Model Set						
Density (kg/m3)	12.2	12.2	24.4	11.9	14.0	12.8
Q gas (m3/sec)	2.325	0.884	0.433	0.343	0.140	0.156
Ts (oK)	313.2	311.2	312.2	19.5	23.0	21.0
Molecular weight	20.0	20.0	20.0	20.0	20.0	20.0
Cp ratio	0.83	0.83	0.90	1.00	1.00	1.00
Tair (oK)	310.2	309.2	299.7	294.5	294.5	294.7
u* (m/sec)	0.374	0.280	0.360	0.454	0.253	0.360
Zo (m)+	0.005	0.005	0.005	0.005	0.005	0.005
Results						
% reduction seen				10-25%	44%	47%
C300 off	28000.0	20000.0	20000.0	3200.0	2028.0	1440.0^
C300 on				2700.0	574.0*	916.0
C1000 off	3050.0	2000.0	2100.0	400.0		
C1000 on				187.0		
C3000 off	410.0		200.0			
C3000 on						

Notes:
* Centerline of cloud did not cross array
^ Estimate from Test 5 using SLAB calculations
\+ Assumed roughness

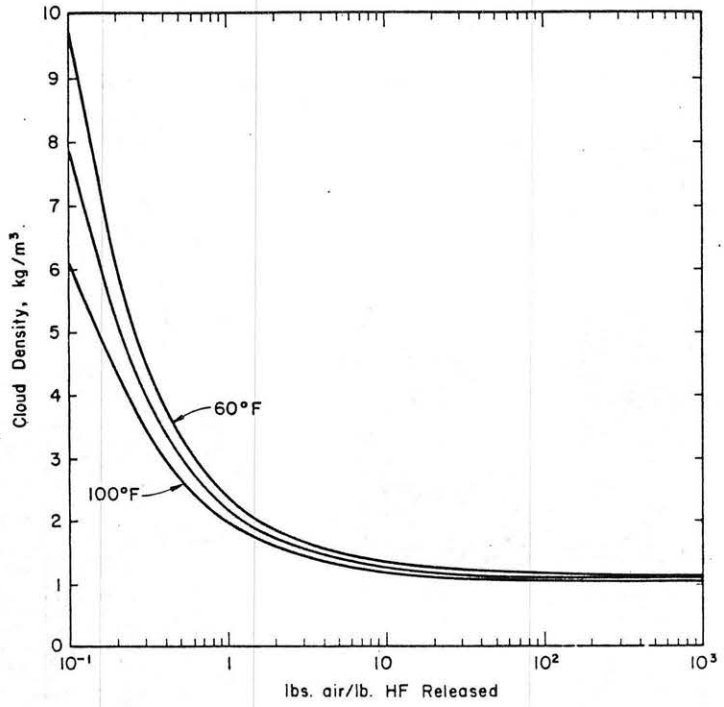

Fig. 2.2-1 Cloud Density vs Air Dilution for VariousInitial Temperatures with 60% Relative Humidity (W. J. Hague, 1988)

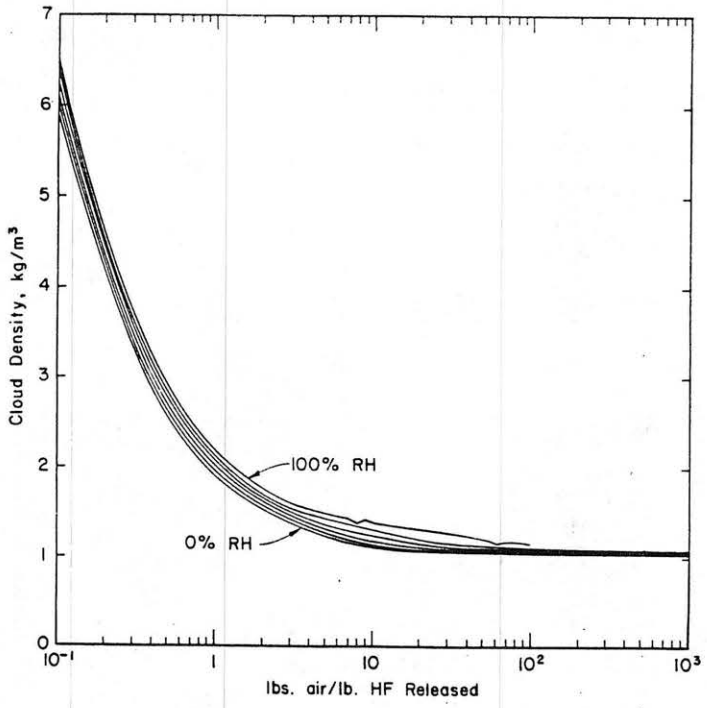

Fig. 2.2-2 Cloud Density vs Air Dilution for VariousHumidity Conditions with Temperatures of 100°F (W. J. Hague, 1988)

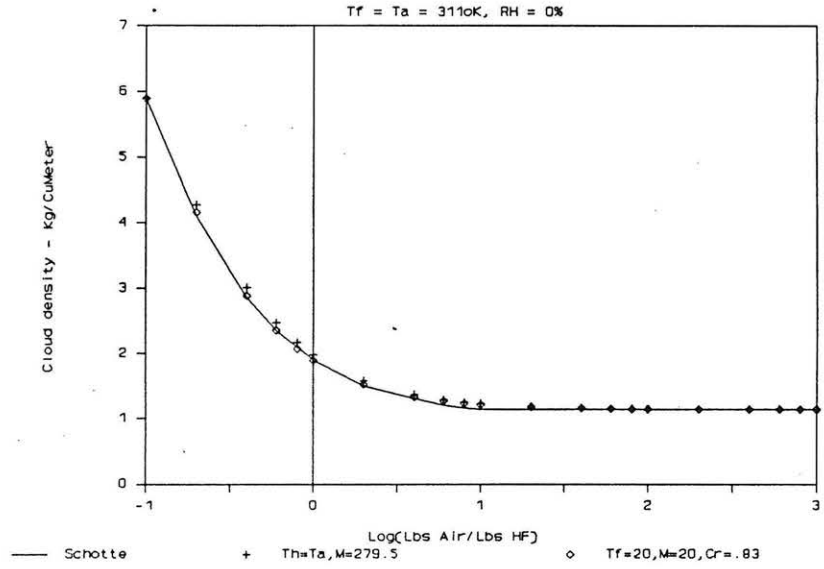

Fig. 2.2-3 Cloud Density vs Air Dilution, Isothermal and Ideal Gas Conditions to Simulate Goldfish Trials 1 and 2

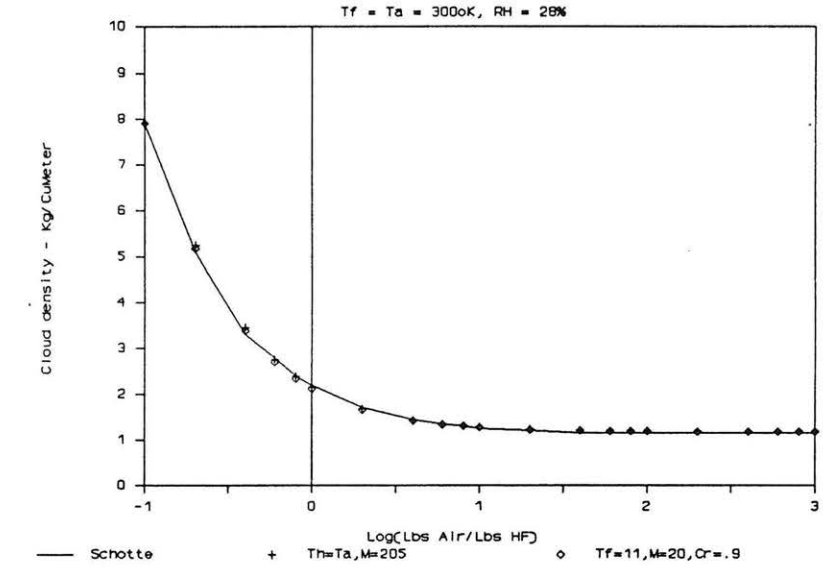

Fig. 2.2-4 Cloud Density vs Air Dilution, Isothermal and Ideal Gas Conditions to Simulate Goldfish Trial 3

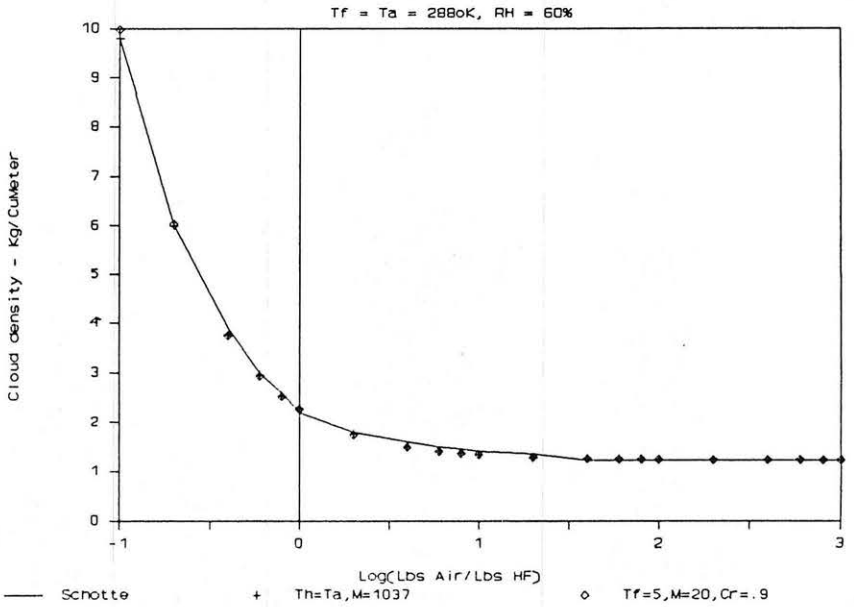

Fig. 2.2-5 Cloud Density vs Air Dilution, Isothermal and Ideal Gas Conditions to Simulate 60% Relative Humidity and Air Temperatures of 15° C

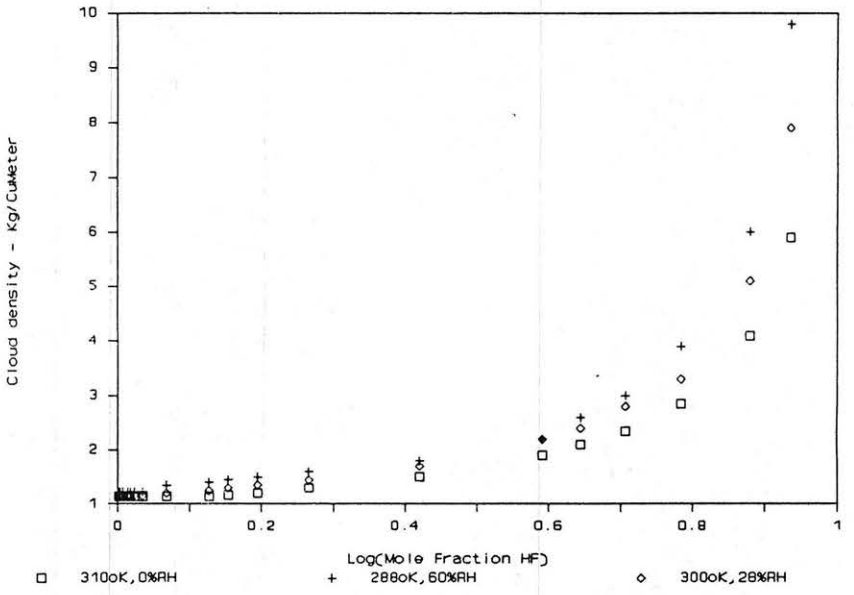

Fig. 2.2-6 Cloud Density vs Mole Fraction, Ideal Gas Simulants

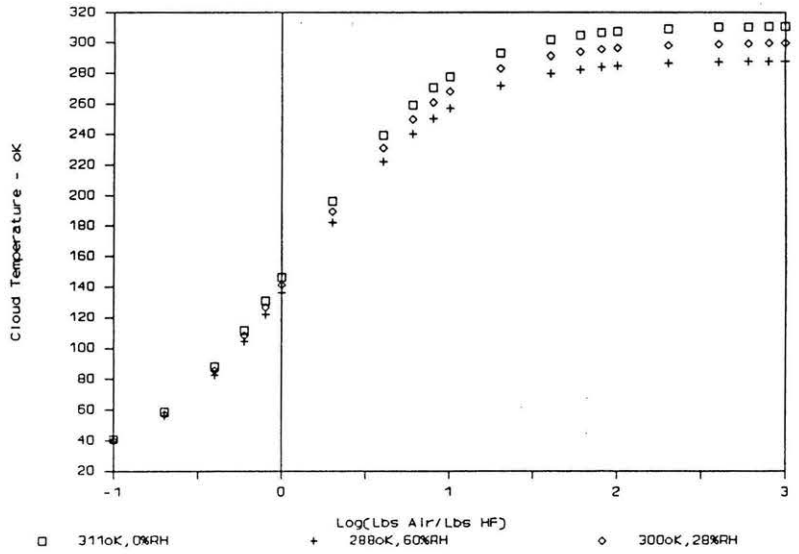

Fig. 2.2-7 Cloud Temperature vs Air Dilution, Ideal Gas Simulants

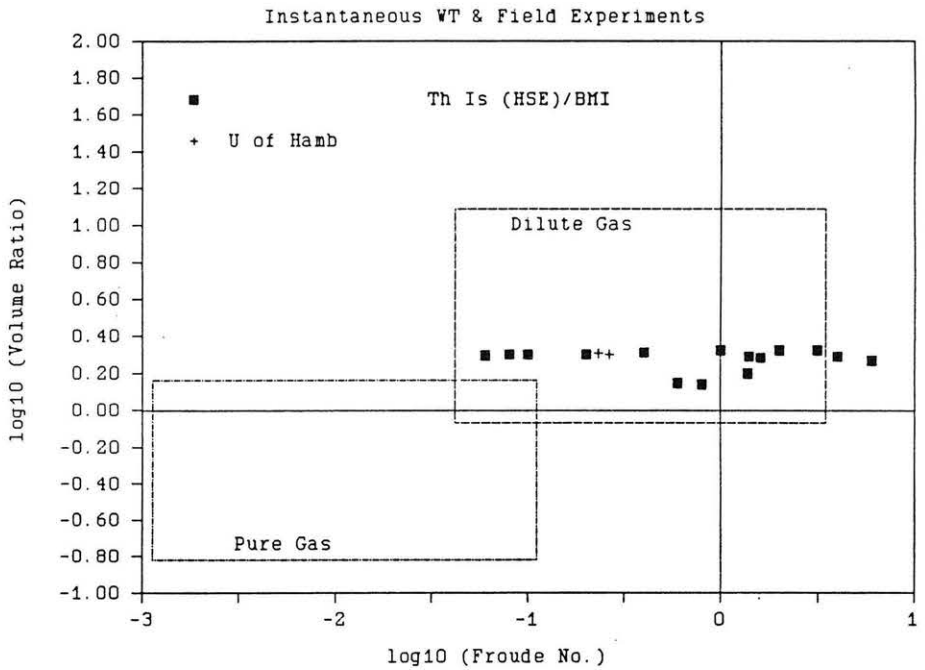

Fig. 2.3-1 Hydrogen Fluoride Accident Envelope, Volume Flux Ratio vs Flux Froude Number, Continuous Spills

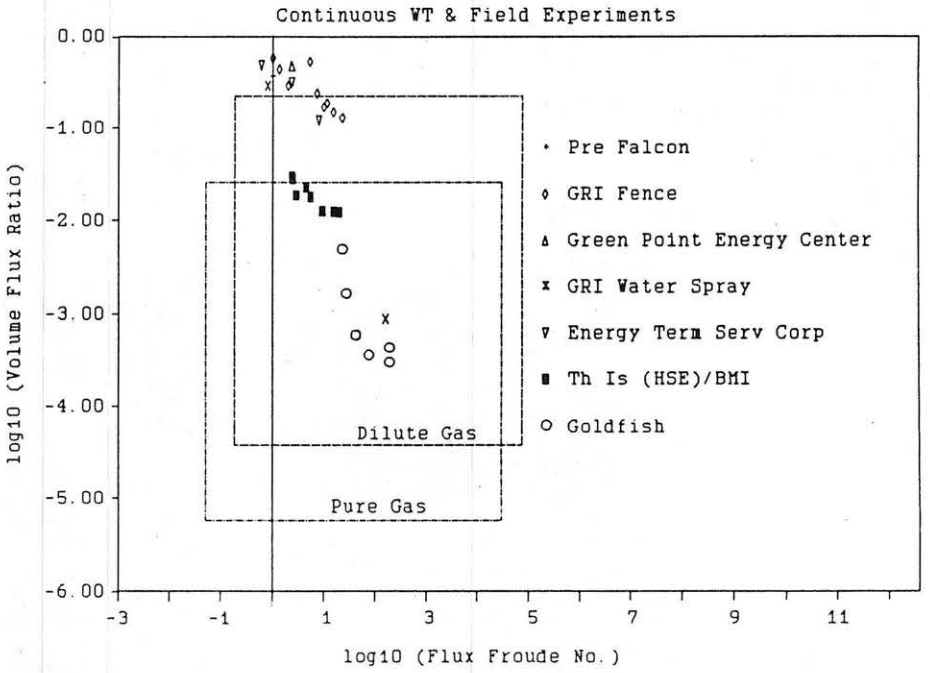

Fig. 2.3-2 Hydrogen Fluoride Accident Envelope, Volume Ratio vs Froude Number, Instantaneous Spills

3.0 APPLICABLE DATA BASES

Puttock, Blackmore and Colenbrander (1982) identified over 22 field experiment programs on dense gas emissions. Subsequently, further field measurements have been performed on the release of Freon-air mixtures at Thorney Island, the release of hydrocarbon fuels at Maplin Sands, and the release of hydrocarbon fuels, ammonia, rocket fuels, and even HF at the DOE Liquefied Gaseous Fuels Test Facility at Frenchman's Flats, Nevada. A number of these experiments have also been simulated in fluid modeling facilities (Meroney, 1986a). This section will identify those experiments relevant to the HF mitigation program for review in Chapter 4.0.

3.1 Field Experiments

The only field experiments performed on the release of HF to the atmosphere seem to be the Goldfish Trials performed by Amoco and LLNL at the DOE test facility (Blewitt et al, 1987a). The parameter values found for the six experiments are noted on Table 2.3-1. The first three trials have been used to validate the numerical models discussed in Chapter 5.1. The second three trials included water spray barrier effects, but, since strong removal of HF by chemical reaction and subsequent deposition occurred, the trials are not considered further in this report.

Phase II and III of the Thorney Island test series included solid fences, porous fences, cubical buildings, and a vapor barrier enclosure (McQuaid and Roebuck, 1984). Some of these tests involved instantaneous release of a cylindrical volume of heavy gas, others permitted continuous release of gas from a point source located a short distance from the cylindrical tent. Thorney Island test cases considered in this report are noted on Table 3.1-1b, Table 4.6-1 and 4.6-2.

During the summer of 1987 LLNL performed a series of five spills of LNG onto a water pond contained within a surrounding vapor barrier fence. During three of these trials substantial disruption of the cloud occurred due to RPT (Rapid Phase Transition) explosions and fire. During one test most of the concentration instrumentation was not operative. During Trial No. 4 a good set of measurements was obtained. Due to the program disruption by the fire a no-barrier case was never completed. Unfortunately, the field data were not available for evaluation during the time of the work effort for this report.

Remember that a single field event has a large number of uncontrolled or poorly specified variables that effect the resultant concentration field. The wind field is normally non-stationary, source flow rates and conditions are typically only approximate, and often the upwind and downwind fetch are non-homogeneous. Evaluation of such data is only possible within the natural limits to predictability permitted by the turbulent nature of the flow fields. Even if it were possible to introduce two separate field plumes into the same resolved wind field, there would be some variance in the dynamics of the two plumes due to the unresolved turbulence. This means that an effort to discriminate between models based on one data set is likely to be unjustified. The best

safeguard against making large modeling errors will be an evaluation methodology which searches for trends across a large set of field experiments.

A summary of some of the wind, site, and source characteristics for each test series is summarized in Table 3.1.

3.2 Laboratory Experiments

Twelve laboratory studies have been identified which included the effects of obstacles, vapor barriers, or fences on the dispersion of dense gas clouds. A summary of some of the wind, site, and source characteristics for each test series is summarized in Table 3.1. The early dense gas tests by Meroney et al. (1976, 1977) were found to be dominated by the large tanks considered, and the gas concentration instrumentation was not as reliable as that used in subsequent experiments. Hence, these experiments were eliminated from further consideration.

Large tanks and dikes were present during the studies by Kothari and Meroney (1980, 1981). Since these tests included complicated surrounding building complexes typical of industrialized areas, the data were examined for gross tank effects on the dense cloud.

Systematic studies of various vapor barriers, vortex generators, and tank arrangements were considered by Kothari et al. (1981) and Kothari and Meroney (1982). Only continuous releases were tested; hence, any effect on plume arrival, peak arrival or departure time could not be evaluated.

Water spray barriers were tested by Meroney et al. (1983, 1984) and Heskestad et al. (1985). One set of model tests replicated the water spray conditions tested during the Health and Safety Executive (HSE) field tests on carbon dioxide dilution (Moodie, Taylor, and Beckett, 1981). (Unfortunately, anemometry was subsequently found to be sheltered by gas tanks during the HSE field experiment, making much of the field data suspect.)

The British Maritime Institute (BMI) modeled the Thorney Island Trials at a variety of model scales and various model parameter assumptions (Davies and Inman, 1986). They replicated each experiment several times, so their data tends to bound the range of behaviors possible in the field. The time series for each measurement location are archived on tape, but have not yet been distributed outside the BMI. Since both field and laboratory data now exist for the Thorney Island Trials, these data were evaluated by the Surface Pattern Comparison technique described by Meroney (1986). Results are considered in Chapter 4.0.

Finally Koenig and Schatzman (1986) performed a variety of model experiments on instantaneous and continuous spills to evaluate the influence of street canyons between tall buildings, street intersections, cross-wind depressions or roadways, and longitudinal walls and fences.

Their data are significant in that they display the potential of obstructions to reduce spread and inhibit mixing.

Table 3.1-1a Data Sets Relevant to HF Mitigation Review

Authors (Date)	Title	Mitigation Devices Studied	Model Scales	Spec. Grav. Low	Spec. Grav. High	Source Type	Source (m3/m) Low	Source (m3/m) High	Boiloff Rate	Zo (m)	Power Law	Wind Speed Low	Wind Speed High	Structure Hts. Low	Structure Hts. High	Structure Wdth Low	Structure Wdth High	Stab.	Total Tests
Meroney et al (1976)	Wind Tunnel Study of the Negatively Buoyant Plume Due to an LNG Spill	High dikes	1:130,200,666		1.4	Area	1583	64279	V		0.23	3	7	24.4	39.3	73.2	79.2	N, S	45
		Low dikes	1:200,666		1.4	Area	3766	60315	V		0.23	3	7	6.4	36.9	93	100.6	N, S	52
Meroney et al (1977)	Dispersion of Vapor from Lng Spills - Simulation in a Meteorological Wind Tunnel	High dikes	1:200,400		1.4	Area	1528	42475	C, V			3.1	7.2		24.4		79.2	N, S	19
		Low dikes	1:400		1.4	Area	3681	39644	C, V			3.1	7.2		6.4	93	100	N, S	9
		AGA Capistrano	1:106		1.4	Area	453	4531	C, V			5.4	5.4		0.6		24.4	N	4
Kothari & Meroney (1980)	Dispersion of Vapor from LNG Spills at Green Point Energy Center: Simulation in a Wind Tunnel	Low dikes	1:400		1.38 4.18	Area	800	64000	Step		0.16	2.23	8.93			100	100	N	141
Kothari & Meroney (1981)	Dispersion of Vapor from LNG Spills at Energy Terminal Service Corporation: Simulation in a Wind Tunnel	Dikes	1:250		1.38	Area	50.8	101.7	C, Step		0.27	2.9	6.69	2.44	4.88	50	410	N	40
		Vapor barrier fences									0.22								
Kothari et al (1981)	LNG Plume Interaction with Surface Obstacles	Tanks	1:250	1	1.38	Area		7593	C	0.04	0.22	4	7		50		50	N	44
		Buildings	1:250	1	1.38	Area		7593	C	0.04	0.22	4	7		18.75		18.75	N	20
		Tree fences	1:250	1	1.38	Area		7593	C	0.04	0.22	4	7		7.5	30%poro	300	N	20
Kothari & Meroney (1982)	Accelerated Dilution of LNG Plumes with Fences and Vortex Generators	Fences	1:250	1	1.38	Area	5062	10124	C			4	12	5	10	75	150	N	84
		Vortex Generators	1:250	1	1.38	Area	5062	10124	C			4	12	5	10	75	150	N	72
Meroney et al (1983)	Model Study of LNG Vapor Cloud Dispersion with Water Spray Curtains	Water spray & Dike	1:5		1.5	Area		8286	C	0.00015			0.5		0.2		3	N	3
		Water spray & Dike	1:100		1.5	Area	3000	21444	C	0.003		2.2	8	0	4		60	N	141
		Water spray & Bldg	1:100		1.5	Area		6000	C	0.003			3	fence 4tank 23fence 6tank 22-36				N	9
Meroney et al (1984)	Wind Tunnel Simulation of Field Dispersion Tests (by UK Health and Safety Executive) of Water-spray Curtains	Water sprays CO2 point source	1:28.9		1.5	Point	22.6	67.9	C	0.0043		1.7	3.2	16	28		36	N	13

Table 3.1-1b Data Sets Relevant to HF Mitigation Review

Authors (Date)	Title	Mitigation Devices Studied	Model Scales	Spec. Grav. Low	Spec. Grav. High	Source Type	Source (m3/m) Low	Source (m3/m) High	Boiloff Rate	Zo (m)	Power Law	Wind Speed Low	Wind Speed High	Structure Hts. Low	Structure Hts. High	Structure Width Low	Structure Width High	Stab.	Total Tests
Heskestad et al (1985)	Dispersal of LNG Vapor Clouds with Water Spray Curtains: Phase 2B: Extended Wind Tunnel Experiments	Water sprays with surfacants	1:100		1.5	Area		6000	C	0.003			3		4		60	N	51
McQuaid & Roebuck (1984)	Large Scale Field Trials on Dense Vapour Dispersion	Unobstructed		0.99	4.2	Volume	1320	2100	Inst			1.7	7.5					C D E F	16
		Buildings		2	4.2	Volume	1850	1950	Inst			1.9	9		9		9	B D E	4
		Fences solid		1.92	4.2	Volume	1400	2000	Inst			1.4	5.9		5		100	C D E F	4
		Fences permeable		1.92	2.03	Volume	1850	1925	Inst			5.8	6.8		10	porous	100	D E	2
		Unobstructed		1.6	2	Point	250	260	C			1.5	3.3					D E F	4
		Tank & Fence		1.4	1.8	Point	185	340	C			1.4	5.8		2.4	25	50	D E F G	13
Davies & Inman (1986)	Wind Tunnel Modelling of the Thorney Island Heavy Gas Dispersion Trials	Unobstructed	1:40,100,150	0.99	4.2	Volume	1320	2100	Inst			1.7	7.5					N	22
		Buildings	1:40,100,150	2	4.2	Volume	1850	1950	Inst			1.9	9		9		9	N	7
		Fences solid	1:40,100,150	1.92	4.2	Volume	1400	2000	Inst			1.4	5.9		5		100	N	6
		Unobstructed	1:40,100,150,	1.6	2	Point	250	260	C			1.5	3.3					N	11
		Tank & Fence	1:40,100,150,	1.4	1.8	Point	185	340	C			1.4	5.8		2.4	25	50	N	37
Neff & Meroney (1986)	LNG Vapor Barrier and Obstacle Evaluation: Wind-tunnel Pre-field Test Results	Fence	1:100		1.38	Area	2208	8826	C			2	5	9.4	14.1	44	88	N	7
		Fence & Vortex generator	1:100		1.38	Area	2208	8826	C			2	5	9.4	14.1	44	88	N	10
Konig & Schatzmann (1986)	Wind Tunnel Modeling of Density Current Interaction with Surface Obstacles	Thrny Is	1:165	1.41	4.18	Volume		2000	Inst		0.16	0	5.7					N	24
		Thrny Is & Fence	1:165	1.41	4.18	Vol or Area		2000	Inst or C		0.16	0	Ucc		5		100	N	15
		Street Canyons	1:165	1.41	4.18	Vol or Area		2000	Inst or C		0.16	0	Ucc						
		Inf long wall																N	12
		Finite long wall																N	12
		Low parallel fences																N	12
		Steet canyon																N	17
		Street crossing																N	2
		Sunken freeway																N	20
		Street canyon 45o																N	8

4.0 RESULTS FROM DATA BASE EVALUATION

The primary purpose of this data review and analysis is to develop general relations that can be used to predict downwind concentrations for different barrier configurations. Concentrations due to a heavy gas release are expected to be a function of some combination of the following dimensionless variables:

Atmospheric Conditions:

Surface roughness coefficient,	Z_o/L_c,
Surface friction coefficient,	u_*/U_{Lc},
Convective velocity coefficient,	w_*/U_{Lc},

Site Configuration:

Barrier dimensions,	H/L_c, W/L_c, and L/L_c,
Water spray gas removal efficiency	Reduction
Water spray rate,	$(w_e)_{spray}/U_{Lc}$,

Spill Characteristics: (Instantaneous):

Froude Number,	$U_{Lc}^2/(g(SG - 1)L_c)$,
Volume Ratio,	$Q/(U_{Lc}L_c^2)$, and
Specific Gravity ratio,	ρ_s/ρ_{air}, or

Spill Characteristics: (Continuous):

Flux Froude Number,	$U_{Lc}^3L_c/(Qg(SG - 1))$,
Volume Flux Ratio,	$Q/(U_{Lc}L_c^3)$, and
Specific Gravity ratio,	ρ_s/ρ_{air},

where the reference wind speed, U, is evaluated at some reference height, L_c. L_c was chosen to be 10 meters at prototype scale for all situations. In some cases the initial momentum of a jet release is also important, but none of the trials examined involved a high velocity source jet.

For each experiment studied the data with a barrier obstacle or water spray has been paired by source Froude numbers and volume release rate with a release without such a barrier (or if a reference case is

missing against a reference barrier situation). Thus, concentration data were examined for variation of the concentration ratio,

$$C_{\text{with barrier}}/C_{\text{no barrier}} = C_w/C_{wo},$$

with other parameters such as downwind distance, X/L_c, etc. Similar consideration was given to cloud arrival time ratio, Ta_w/Ta_{wo}, peak concentration arrival time ratio, Tpa_w/Tpa_{wo}, and departure time ratio, Tda_w/Tda_{wo}. Cloud arrival and departure times were generally chosen to be defined as the time when the concentration first reaches 1% or drops below 1%, respectively (In some cases arrival and departure times were related to the appearance of concentration levels equal to 10% of peak values measured at the sampling point). Drift in base line zero concentration was considered in the selection of peak concentrations and times.

Vertical concentration profiles of peak concentrations for comparable pairs have been plotted where available.

Two sets of data were selected for additional evaluations. Surface pattern comparisons were made between the Thorney Island Trials field data (McQuaid and Roebuck, 1984) and the BMI laboratory tests (Davies and Inman, 1986). A multiple regression ANOVA was applied to selected data from the pre-Falcon test series (Neff and Meroney, 1986).

4.1 Dispersion of Vapor from LNG Spills at Green Point Energy Center: Simulation in a Wind Tunnel," Kothari and Meroney, 1980

Experiment Configuration:

A 1:400 scale model of the Greenpoint Energy Center (GEC) tank farm located in Brooklyn, NY, was placed in the Environmental Wind Tunnel (EWT) at Colorado State University (CSU) to determine the dispersion of LNG spills from an accidental release under neutral atmospheric conditions. LNG dispersion about GEC tank number two was examined for three wind speeds (5, 12.3 and 20 mph), for spills simulating boiloff from partial and full tank spills onto soil and insulated dike surfaces.

Six pairs of measurements were selected for barrier effects evaluation. Reference Tests 145, 146, 147, 148, 149, and 150 were compared with Tests 4, 5, 6, 7, 8, and 9, which included a tank and surrounding dike. Lateral traverses of ground level concentrations at two downwind locations, 122 m and 269 m were reported (Figure 4.1-1).

Results of Comparison:

Lateral concentration ratio profiles at 121.8 m (Figures 4.1-2, 3, & 4) for continuous spills and instantaneous spills onto soil and insulation display an average reduction in centerline concentrations of about 50%, whereas profiles at 269 m (Figures 4.1-5, 6, & 7) suggested average reductions of at most 20%. At the lateral edges of the cloud the barriers cause wider plumes; hence concentration ratios generally exceed 1.0. LNG boiling at slower rates off the insulated dike showed smaller reductions in concentration ratio. For many locations the concentration ratios are highly irregular, sometimes exceeding 2 or 3 along the center of the plume. Cross-wind asymmetries in cloud concentrations are caused by the non-homogeneous velocity field produced by wind flow over the tank-farm complex. Such variations may be considered typical of such non-idealized source conditions.

Time ratios did not exhibit any systematic variation from 1.0 for arrival time, peak time or departure time.

Conclusions:

Peak concentration ratios decrease along plume centerline directly downwind of a dike, but ratios increase at plume edges as the barrier forces spread laterally. No systematic effect of the dike on time ratios could be detected.

There were no systematic variations noted with wind speed or source strength; however, boiloff from the insulated dike showed the least systematic deviations.

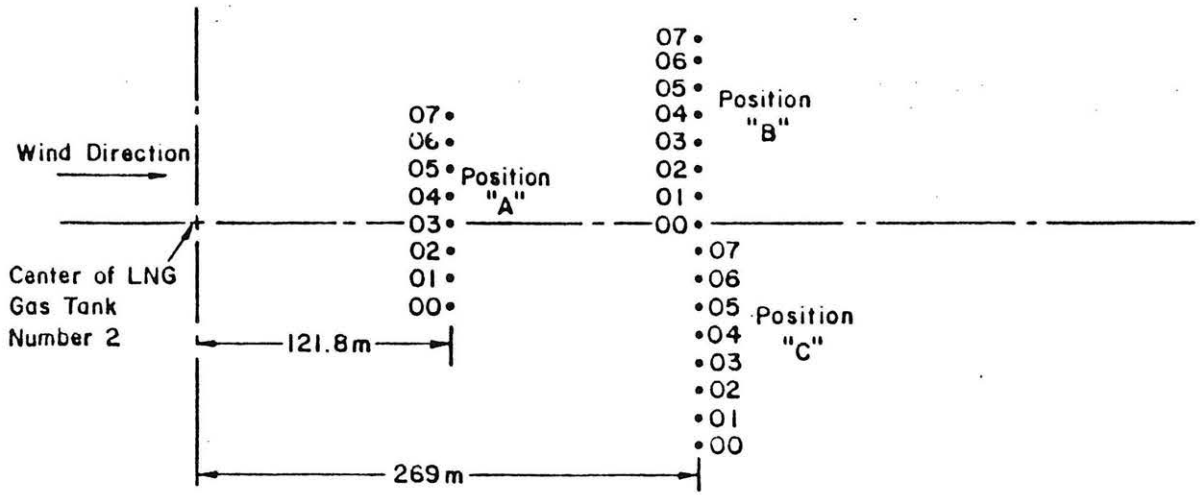

Lateral Distance between Sampling Points = 20m

Source Gas = Argon

Not to Scale

Note: Longitudinal Distance for Rack Position "B" and "C" for Run Numbers 49, 50, 51, 52, 53, 54, 67, 68, 69, 70, 71, and 72 was 223m instead of 269m.

Figure 4.1-1 Experimental Configuration and Measurement Grid, Green Point Energy Center

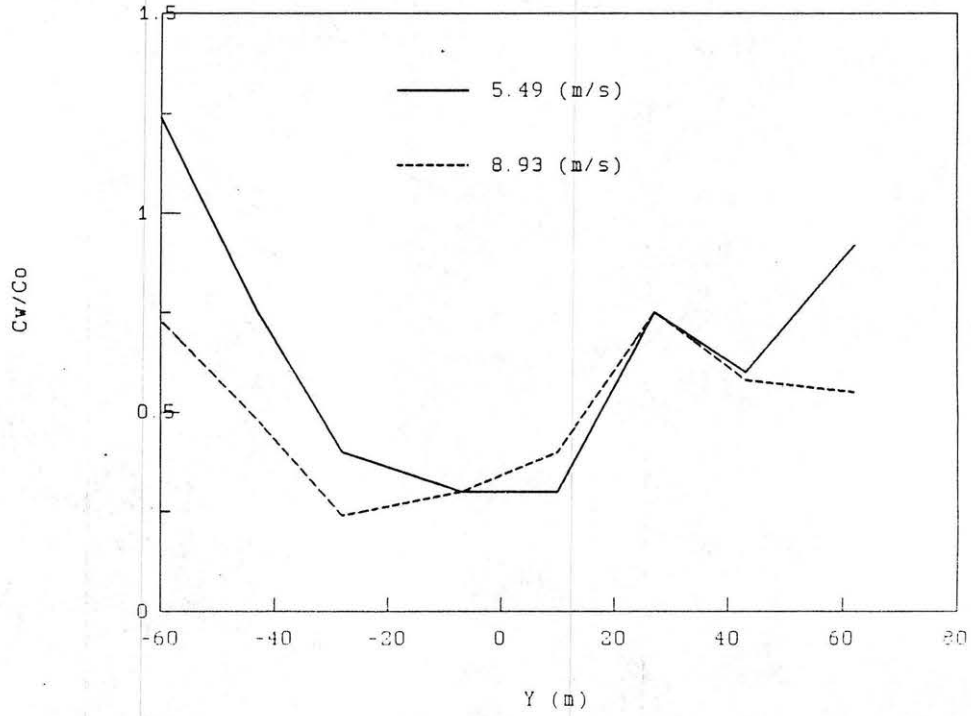

Fig. 4.1-2 Peak Concentration Ratio vs Crosswind Distance at X = 122 m, Continuous Spill at Green Point Energy Center

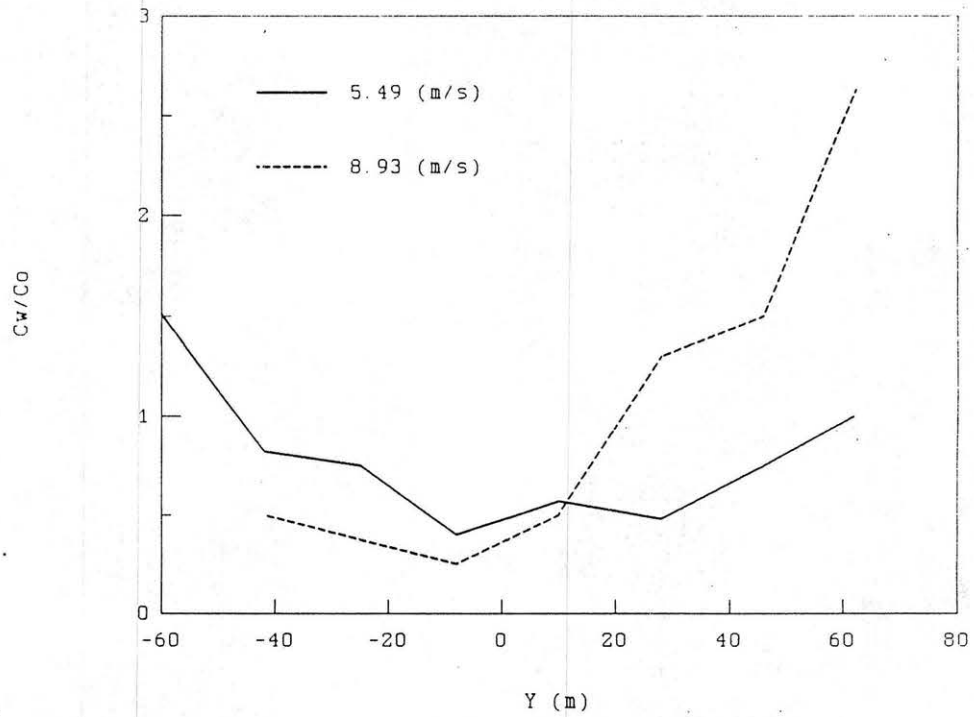

Fig. 4.1-3 Peak Concentration Ratio vs Crosswind Distance at X = 122 m, Instantaneous Spill onto Soil Dike Floor at Green Point Energy Center

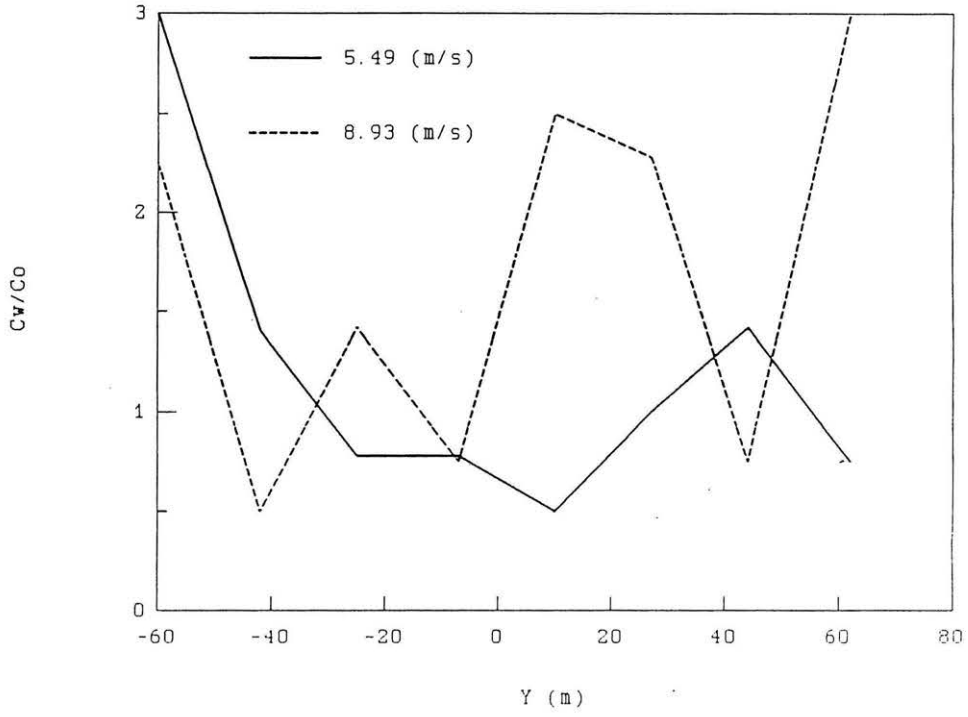

Fig. 4.1-4 Peak Concentration Ratio vs Crosswind Distance at X = 122 m, Instantaneous Spill onto Insulated Dike Floor at Green Point Energy Center

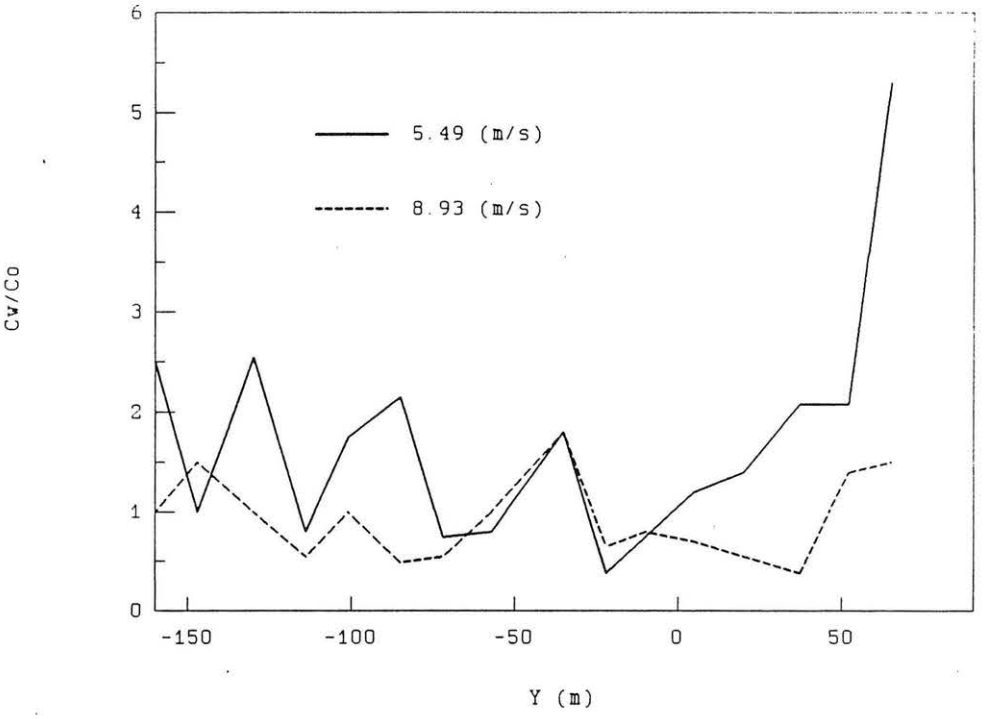

Fig. 4.1-5 Peak Concentration Ratio vs Crosswind Distance at X = 269 m, Continuous Spill onto Soil Dike Floor at Green Point Energy Center

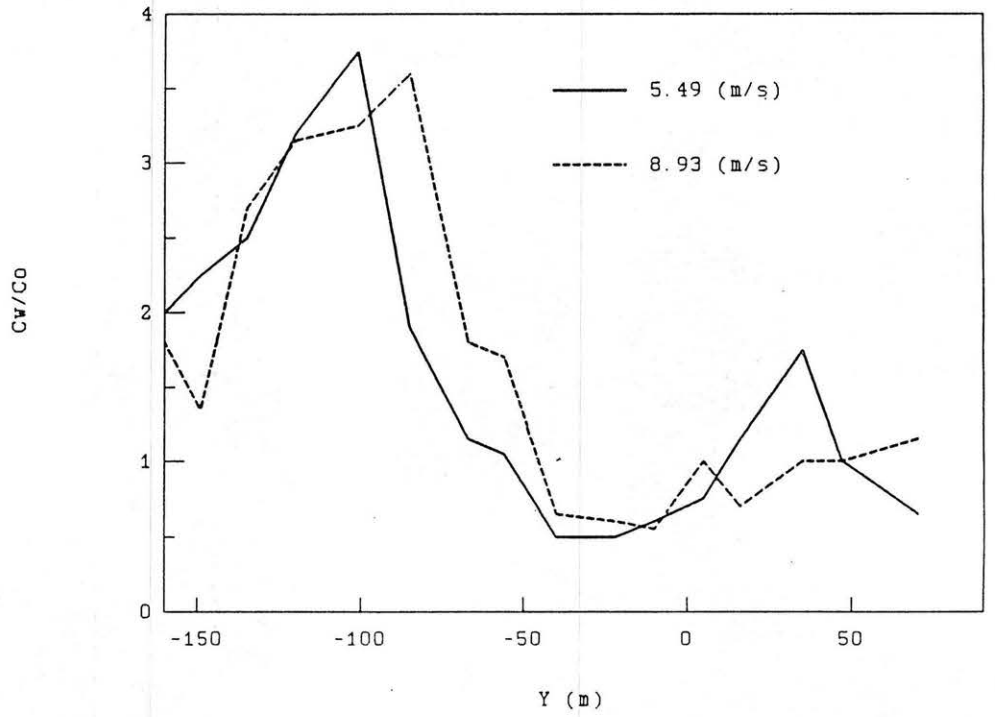

Fig. 4.1-6 Peak Concentration Ratio vs Crosswind Distance at X = 269 m, Instantaneous Spill onto Soil Dike Floor at Green Point Energy Center

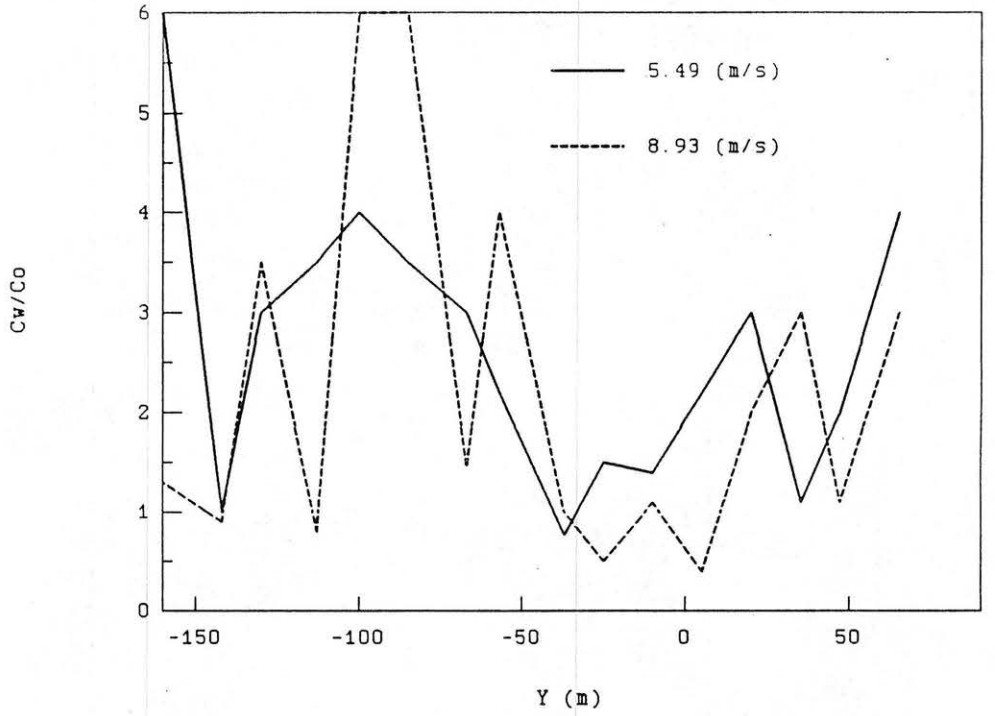

Fig. 4.1-7 Peak Concentration Ratio vs Crosswind Distance at X = 269 m, Instantaneous Spill onto Insulated Dike Floor at Green Point Energy Center

4.2 Dispersion of Vapor from LNG Spills at Energy Service Terminal Corporation: Simulation in a Wind Tunnel," Kothari and Meroney, 1981

Experiment Configuration:

A 1:250 scale model of the Energy Terminal Service Corporation (ETSC) facility at Staten Island was placed in the EWT at CSU to study the dense gas cloud behavior resulting from an accidental LNG release under neutral stability. A total of three wind speeds, five LNG release locations, three wind directions, two boiloff rates for unlimited spill duration, one boiloff rate for 10 minutes spill duration, and three vapor barrier fence heights were investigated. Since all tests were performed in the presence of large storage tanks and vapor barriers, shorter fences in Runs 1, 3, 5, 7, 9, 11, 31, and 33 were compared against taller fences but otherwise equivalent situations in Runs 2, 4, 6, 8, 10, 12, 32, and 34 (See Table 4.2-2).

Results of Comparison:

For a wind direction of 315° (wind directly over the large storage tanks; Figures 4.2-1 & 2) an increase of vapor barrier height from 2.44 to 4.88 m produced up to 70% reduction in concentrations near the fence (circa 10 to 25 m; Figures 4.2-3 & 4) and no significant decrease further from the fence (circa 30 to 50 m; Figure 4.2-5). No significant trend was noted for different wind speeds.

For a wind direction of 270° (wind at 45 degrees to the line connecting the two storage tanks; Figures 4.2-6) an increase of vapor barrier height from 2.44 to 4.88 m produced inconsistent results. In one set of measurements a wind speed of 4.46 m/sec produced concentration reductions of 40% and a wind speed of 6.69 m/sec produced no significant improvement; but in the other measurements just the opposite trend was observed (Figure 4.2-7 versus 4.2-8).

For a wind direction of 215° (wind passes over the process area parallel to the storage tanks; Figure 4.2-9) an increase of vapor barrier height from 2.44 to 4.88 m produced 40 to 50% reduction in concentration ratios at a location 25 m downwind of the fence (Figure 4.2-10), a reduction of 20 to 40% reduction at a location 50 m downwind of the fence (Figure 4.2-11), and no consistent results at a location 75 m downwind of the fence (Figure 4.2-12). No consistent dependence upon wind speed was noted.

For a wind direction of 215° for a release from area P^* (the north end of area P has been removed) noted on Figure 4.2-13 an increase of vapor barrier height from 4.88 m to 7.32 m produced 20% to 40% reduction in concentration ratio at locations 50 m downwind of the fence (Figure 4.2-14), and a reduction of 20% to 50% at locations 75 m downwind of the fence (Figure 4.2-15). Again no consistent trends with wind speed are discernable.

Conclusions:

For a variety of wind speeds, obstacle orientations, and spill areas a doubling in height of the vapor fence resulted in 20 to 40% reduction in concentrations at distances of x/Href = 5 to 15, and minimal reductions at distances of x/Href > 20.

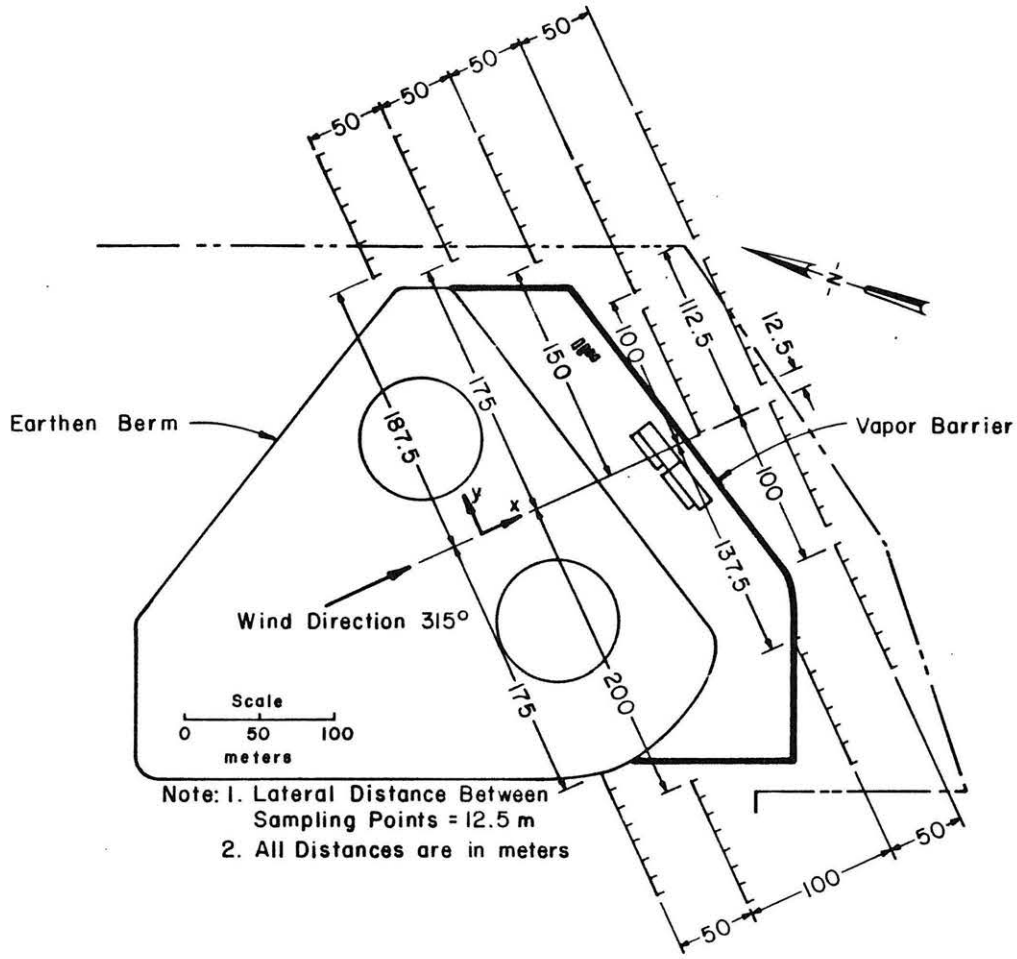

Fig. 4.2-1 Experimental Configuration and Measurement Grid, 315°, Energy Terminal Service Corporation

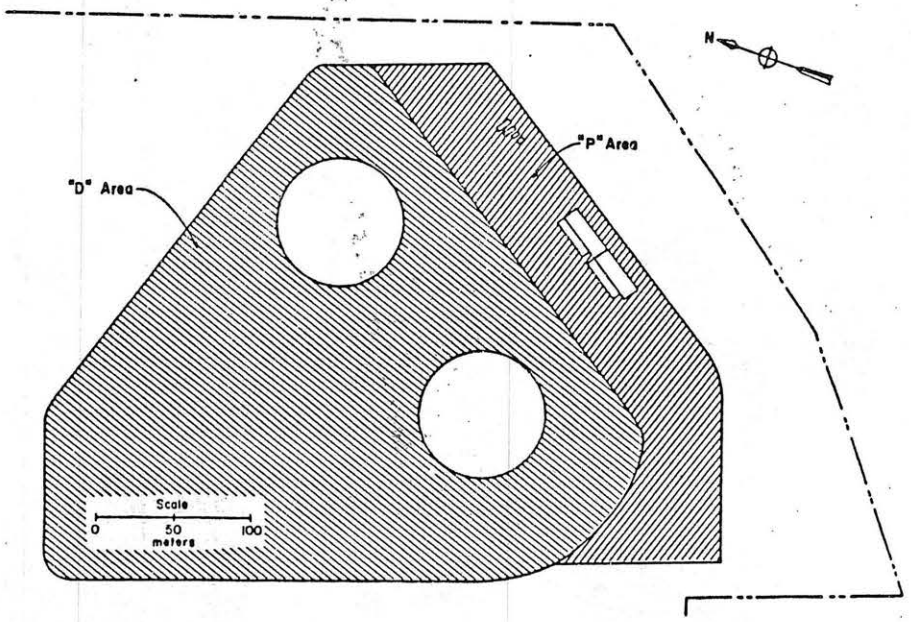

Fig. 4.2-2 LNG Release Areas "P" and "D", Energy Terminal Service Corporation

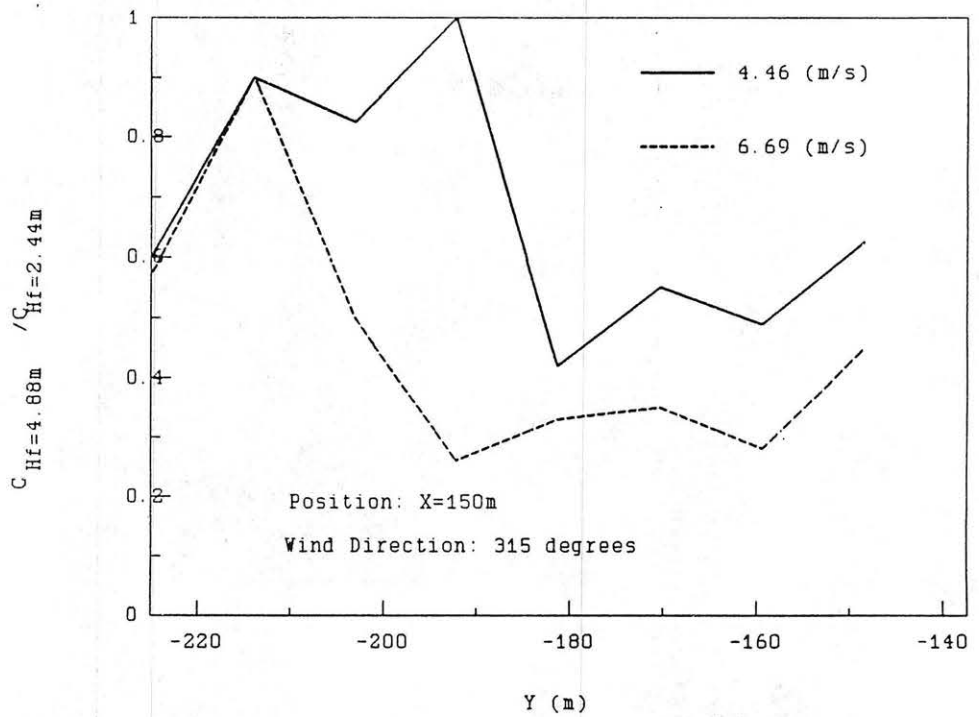

Fig. 4.2-3 Peak Concentration Ratio vs Crosswind Distance, Energy Terminal Service Corporation

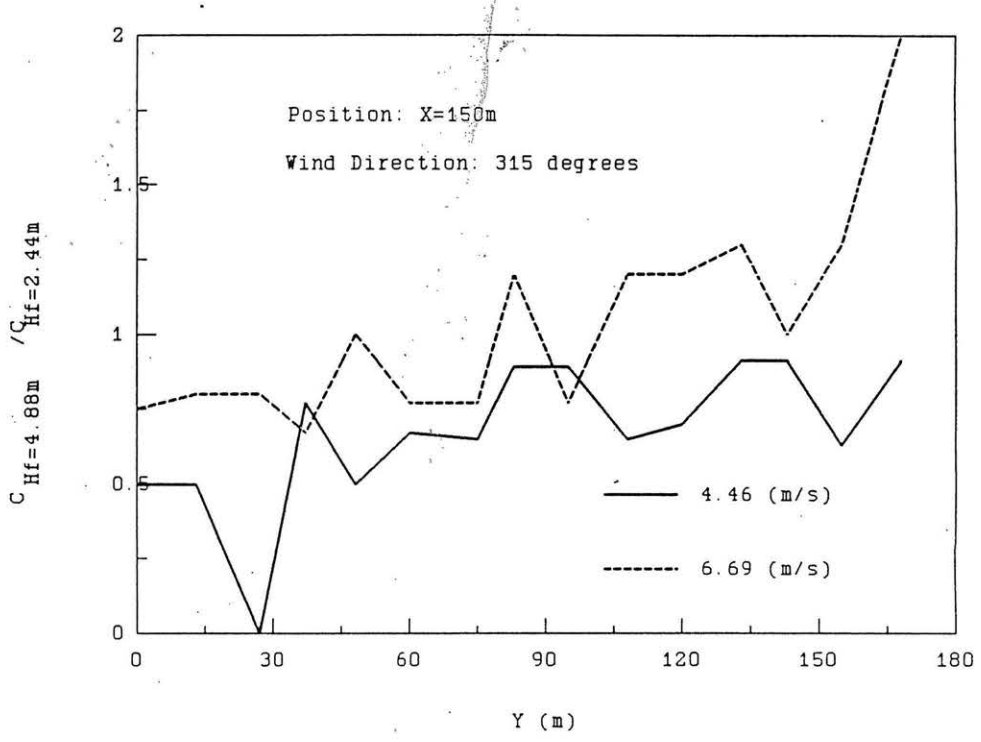

Fig. 4.2-4 Peak Concentration Ratio vs Crosswind Distance, Energy Terminal Service Corporation

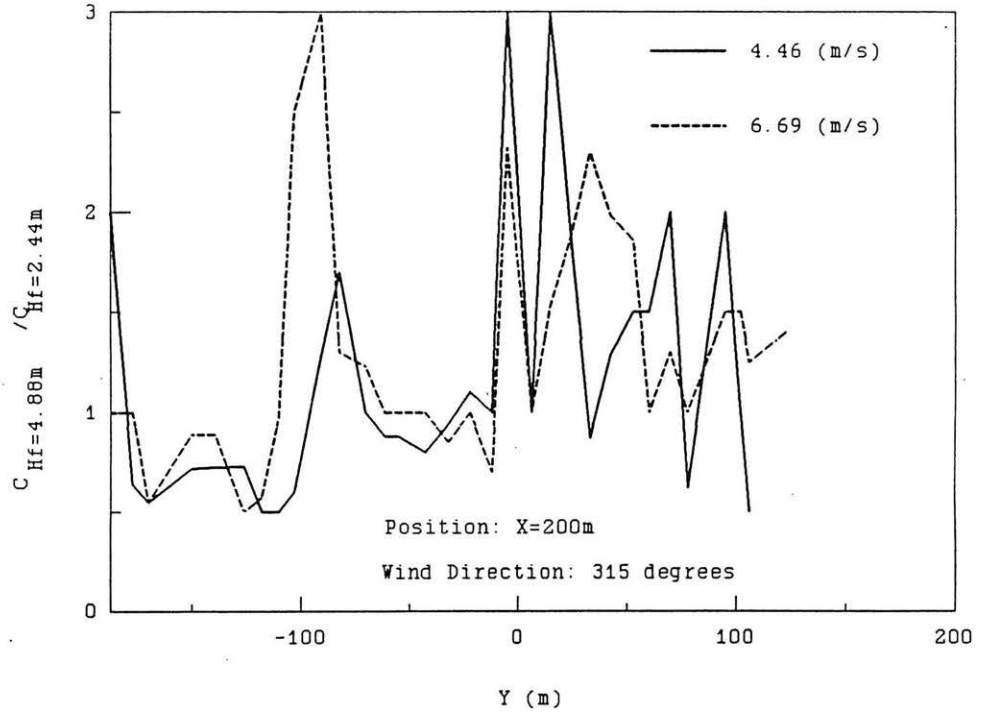

Fig. 4.2-5 Peak Concentration Ratio vs Crosswind Distance, Energy Terminal Service Corporation

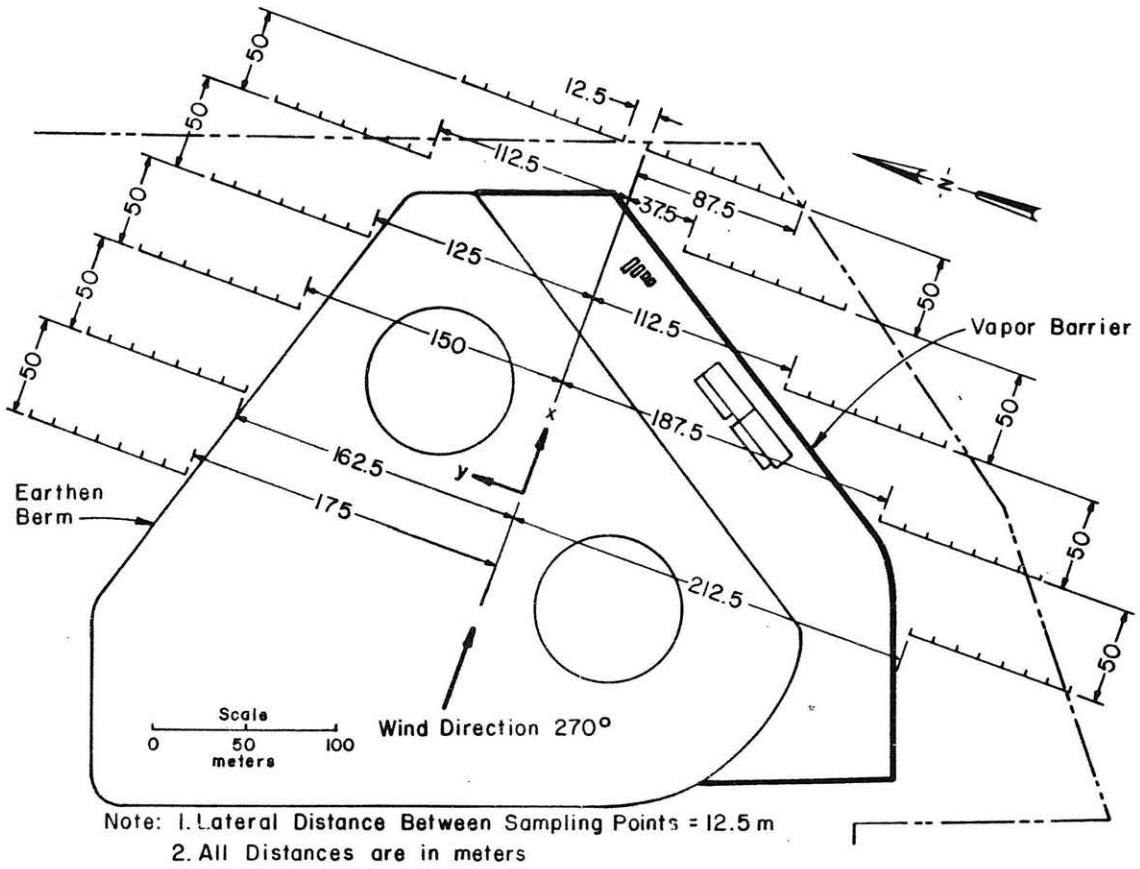

Fig. 4.2-6 Experimental Configuration and Measurement Grid, 270°, Energy Terminal Service Corporation

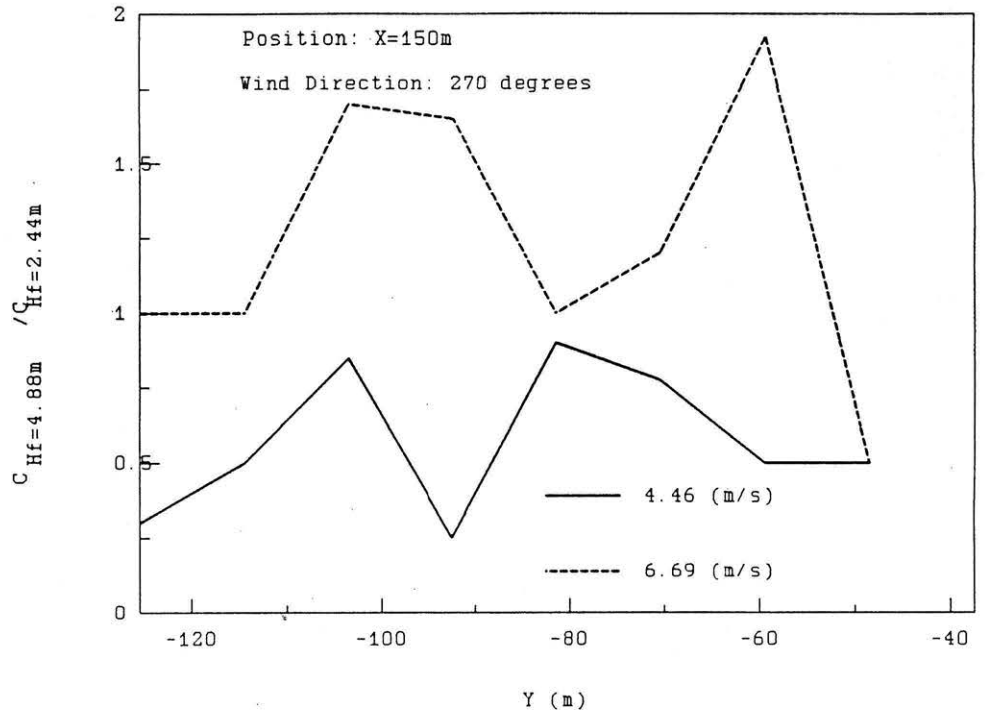

Fig. 4.2-7 Peak Concentration Ratio vs Crosswind Distance, Energy Terminal Service Corporation

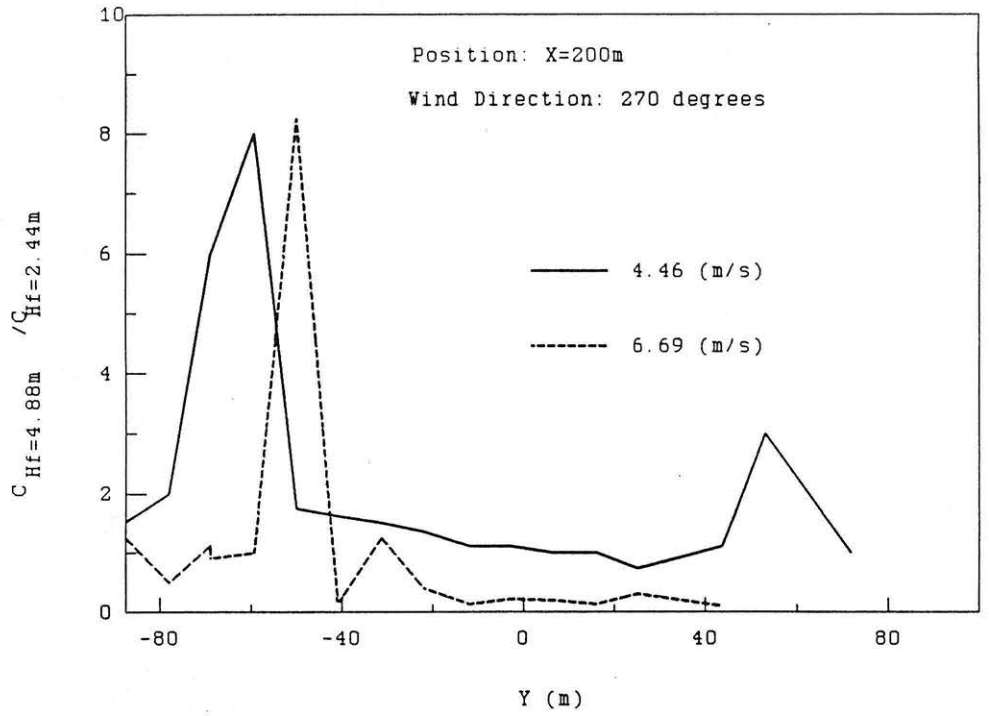

Fig. 4.2-8 Peak Concentration Ratio vs Crosswind Distance, Energy Terminal Service Corporation

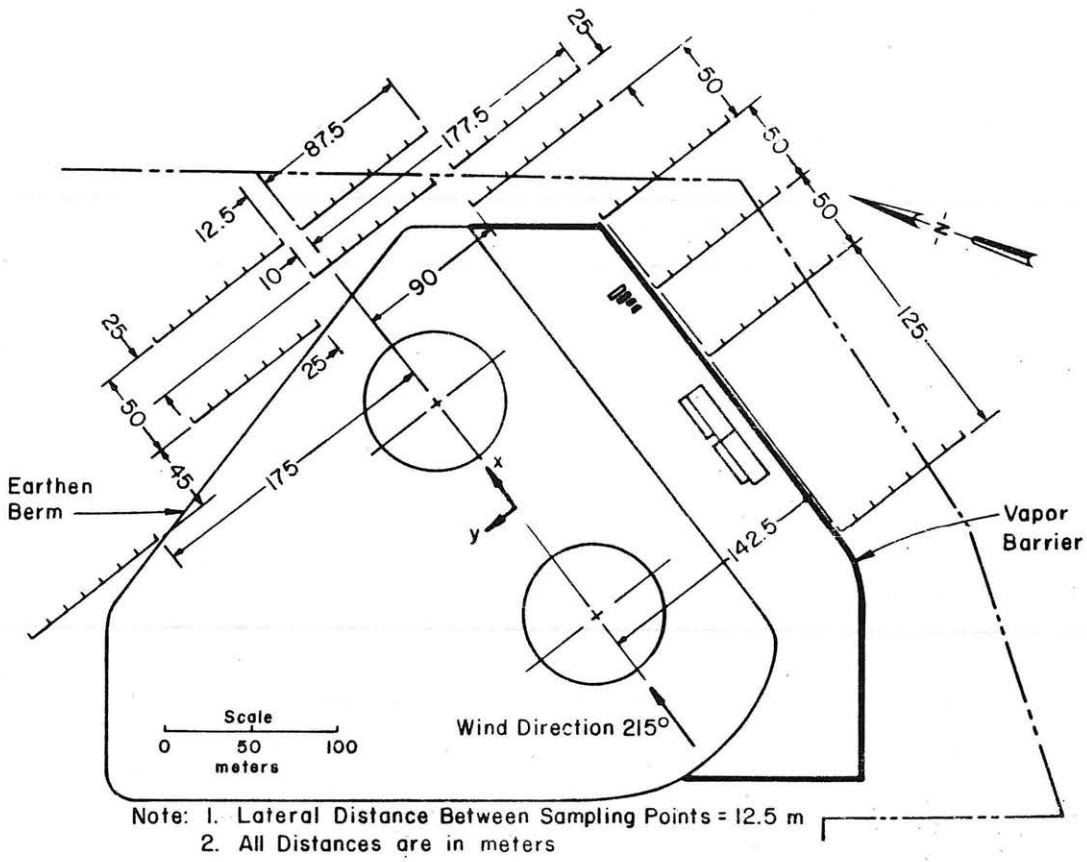

Fig. 4.2-9 Experimental Configuration and Measurement Grid, 215°, Energy Terminal Service Corporation

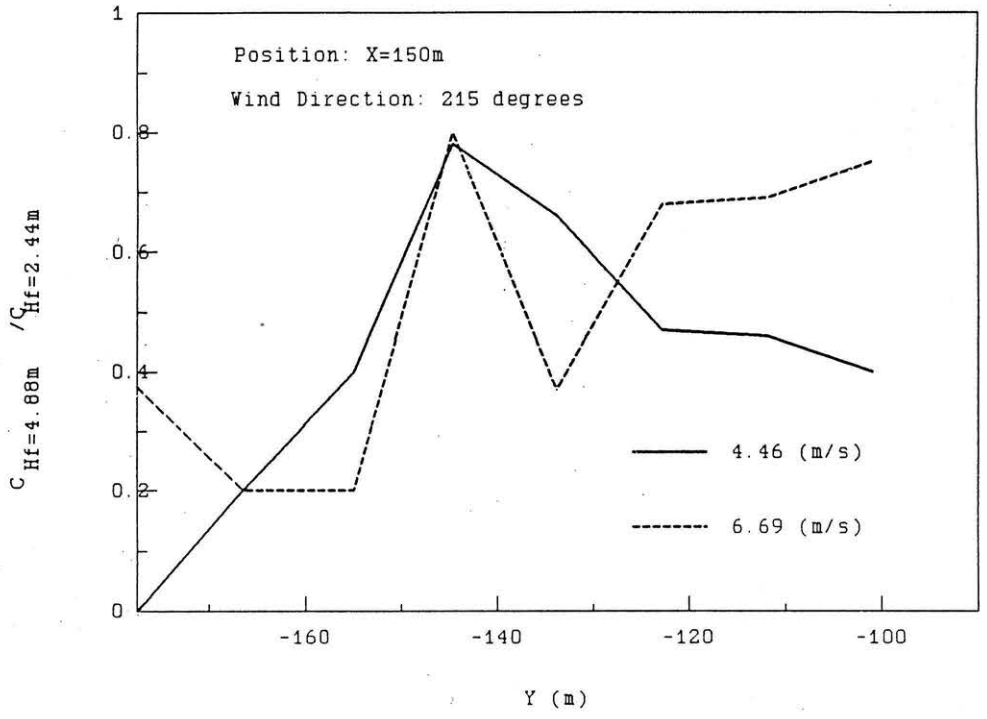

Fig. 4.2-10Peak Concentration Ratio vs Crosswind Distance, Energy Terminal Service Corporation

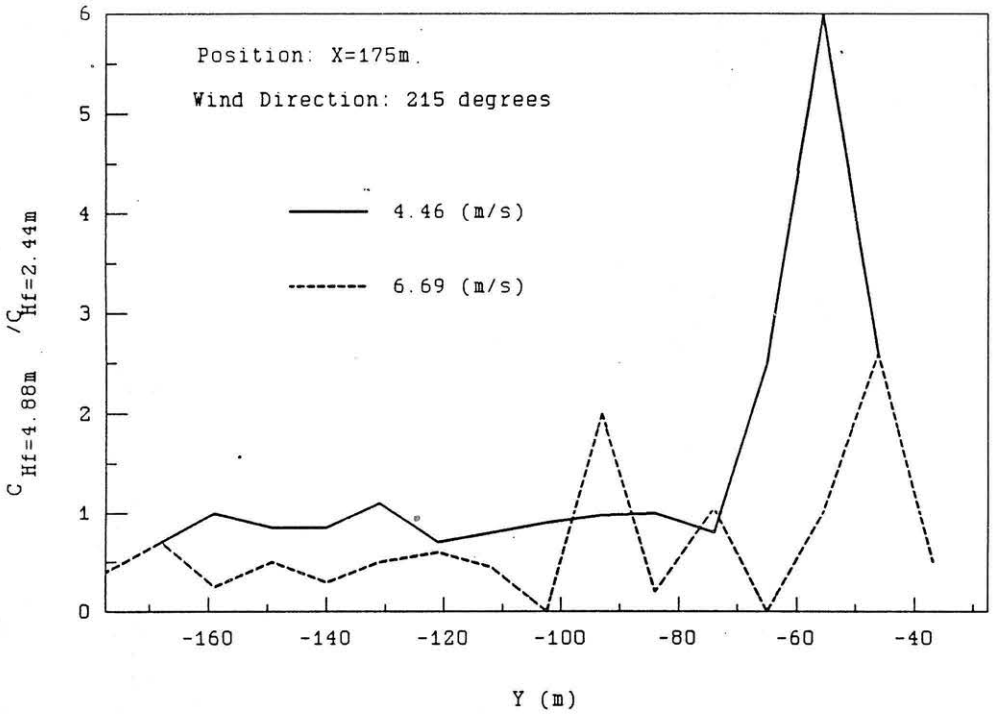

Fig. 4.2-11Peak Concentration Ratio vs Crosswind Distance, Energy Terminal Service Corporation

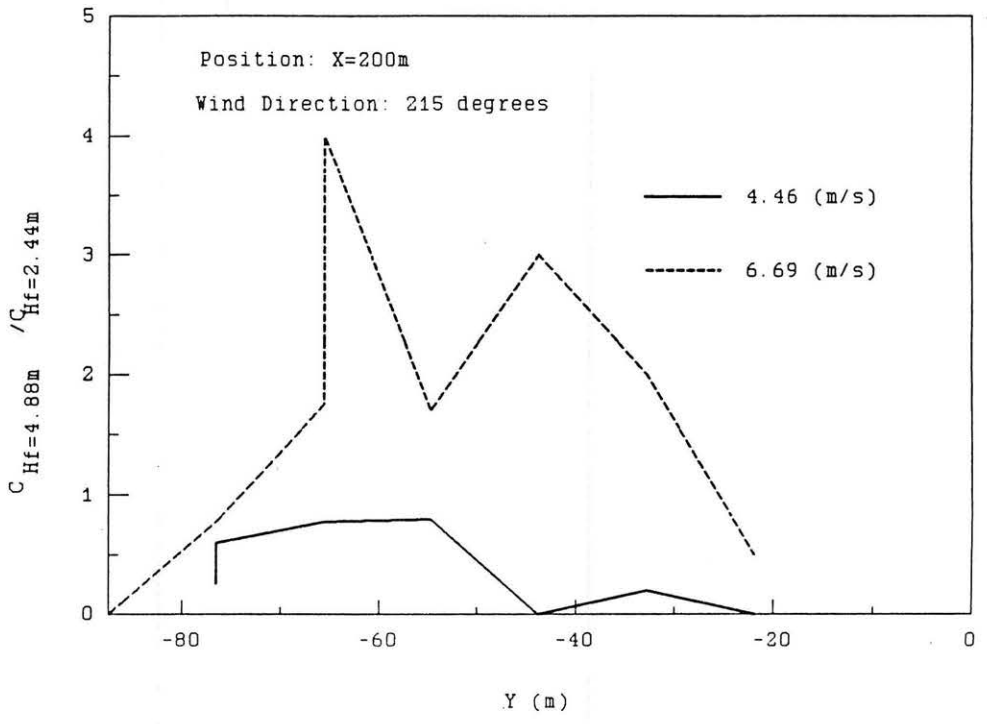

Fig. 4.2-12Peak Concentration Ratio vs Crosswind Distance, Energy Terminal Service Corporation

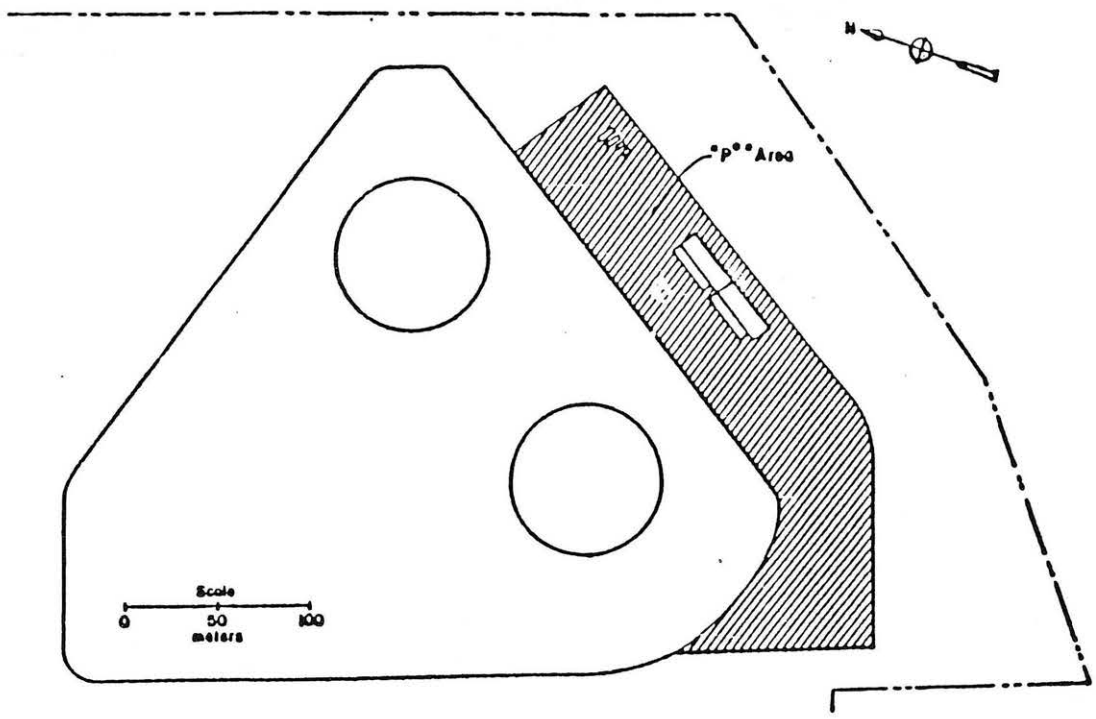

Fig. 4.2-13 Experimental Configuration and Measurement Grid, 215°, Source Area P*, Energy Terminal Service Corporation

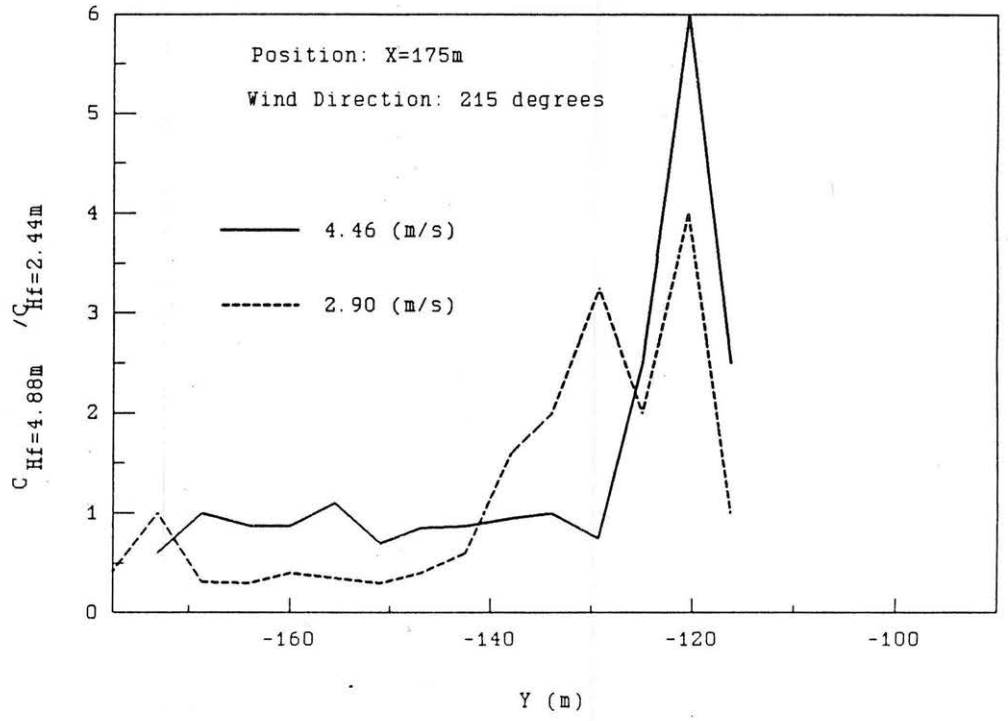

Fig. 4.2-14Peak Concentration Ratio vs Crosswind Distance, Energy Terminal Service Corporation

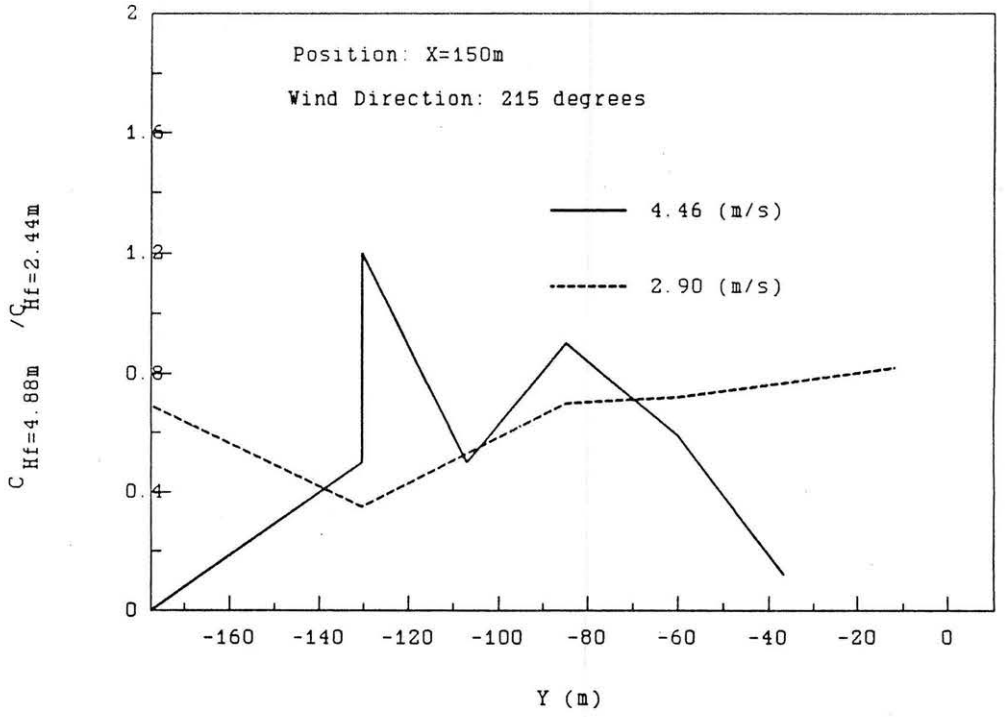

Fig. 4.2-15Peak Concentration Ratio vs Crosswind Distance, Energy Terminal Service Corporation

4.3 "LNG Plume Interaction with Surface Obstacles," Kothari, Meroney, and Neff, 1981

Experiment Configuration:

A wind-tunnel test program was conducted for dense gas dispersion over 1:250 scale models of tanks, buildings, and tree rows placed up and downwind from an LNG release point. One wind direction, two wind speeds (4 and 7 m/sec) and one spill rate (30 cubic meters/min LNG boiling continuously from a 75 m pool) were investigated for neutral and dense source gases. Twenty-two arrangements of tanks, buildings and tree fences were examined (Figures 4.3-1a to 4.3-1e). Tanks, buildings and tree lines had heights of 50, 18.75 and 7.5 meters respectively. Surface concentrations were measured over a grid ranging from 100 to 750 m downwind of the release point (Figure 4.3-1a). A total of 44 tests were performed using a flame-ionization detector (FID) or an aspirated hot-wire katherometer (AHWK). The AHWK was used to measure fluctuating concentration measurements; hence, the report includes tables of rms and peak concentration data.

Results of Comparison:

Ratios of centerline peak concentration with and without the configuration obstacles were plotted versus downwind distance for each test case. As noted on Figure 4.3-2 higher wind speeds generally resulted in greater mitigation rates. When the tank was placed directly over the source the peak concentration ratios fell to a minimum between 0.05 to 0.3 at 3 to 4 obstacle heights downwind of the source, then the ratio began to increase with downstream distance. Eventually the ratio is expected to approach 1.0 at distances exceeding several kilometers.

When the obstacle is placed farther upwind of the spill point mitigation is less; however, dilution increases with the size and number of surrounding obstacles (Figure 4.3-3). A minimum ratio usually occurred some 4 to 6 obstacle heights from the source, even when the obstacle was placed upwind. Obstacles placed downwind of the source reduced concentrations slightly upwind of the obstacle, but the major reduction occurred immediately downwind of the object (Figure 4.3-4). The most reduction in peak concentrations appeared to occur when the obstacles were located between 1 obstacle height upwind or downwind of the spill center. (Figure 4.3-5a and 4.3-5b).

The 7.5 m tree line of 30% porosity placed 75 m downwind of the source produced significant plume dilution. Concentration ratios consistently fell below 0.2 and often as low as 0.025 at 15 fence heights downwind of the tree line (Figure 4.3-6).

Conclusions:

For a variety of wind speeds, obstacle types, and obstacle orientations reductions in plume concentrations were measured in the wake of the objects. Maximum dilution occurred when the objects were placed

close to the spill, but dilution continued to occur even when the object was downwind of the release location. Obstacles need not be large (tall) to produce concentration reductions, but they are more effective when distributed laterally across the plume path (i.e. buildings and tree line). Although most measurements were made in the near field to the source (i.e. less than 15 tank heights downwind), there was some evidence that the peak concentration ratio increases after reaching a minimum some 3 to 4 obstacle heights downwind of the release point.

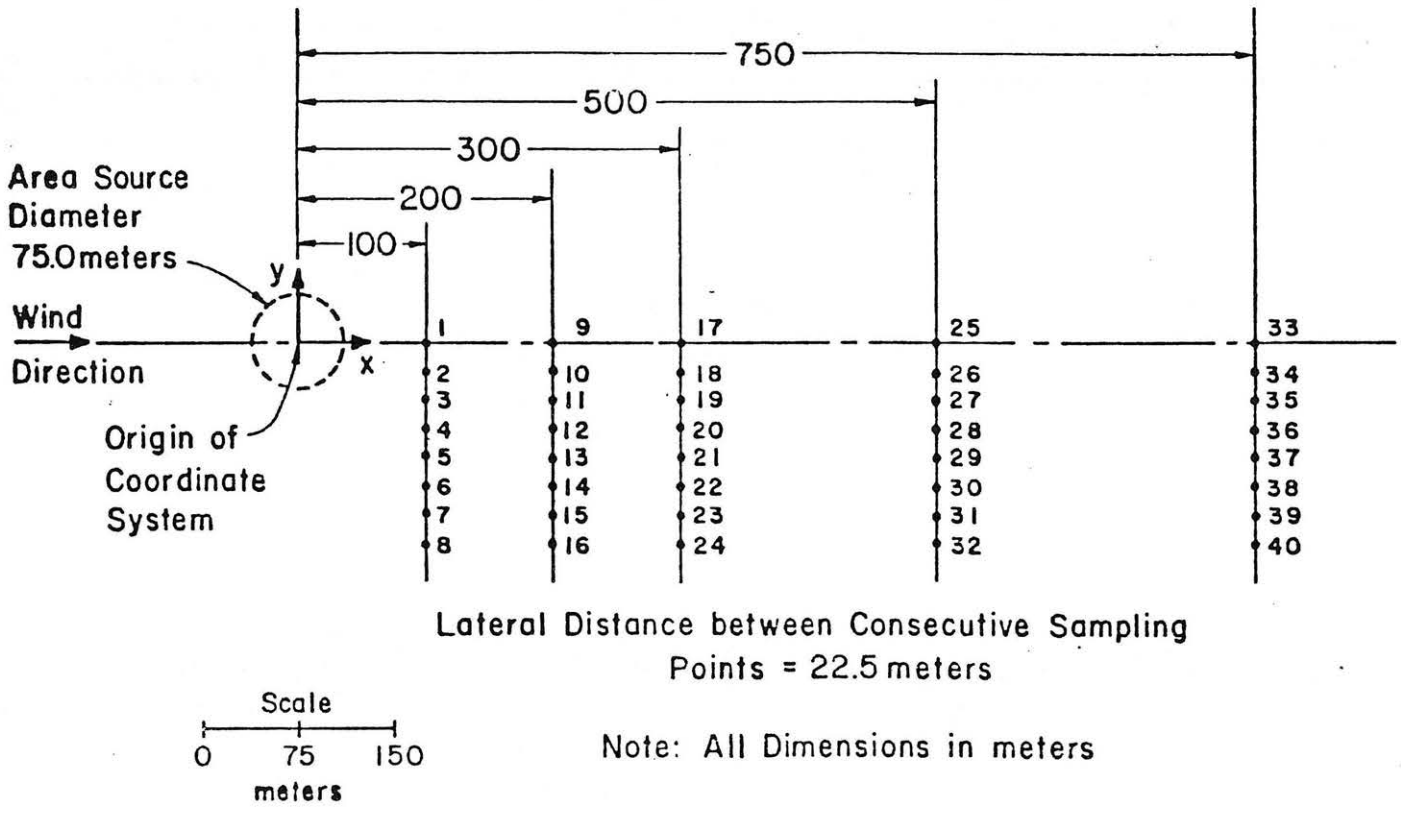

Fig. 4.3-1a Concentration Measurement Locations and Configuration 1 - 22 Spill Arrangement

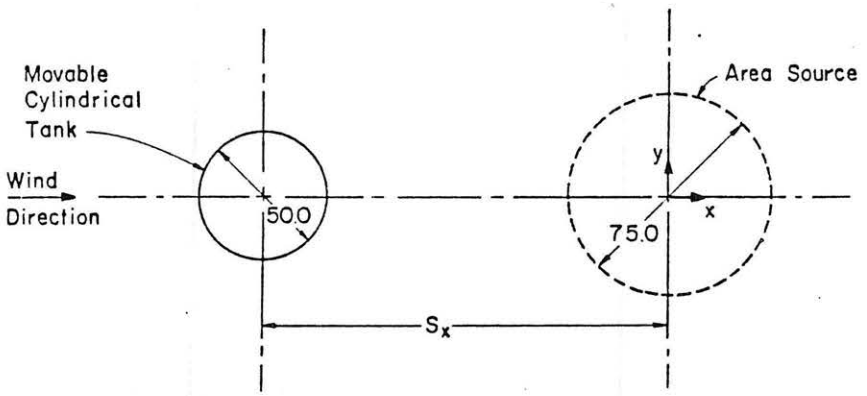

Configuration	Displacement in x Direction S_x, meters
2	0.0
3	-250.0
4	-150.0
5	-50.0
6	50.0
7	150.0
8	250.0

Note: All Dimensions in meters

Fig. 4.3-1b Concentration Measurement Locations and Configuration 1 - 22 Spill Arrangement

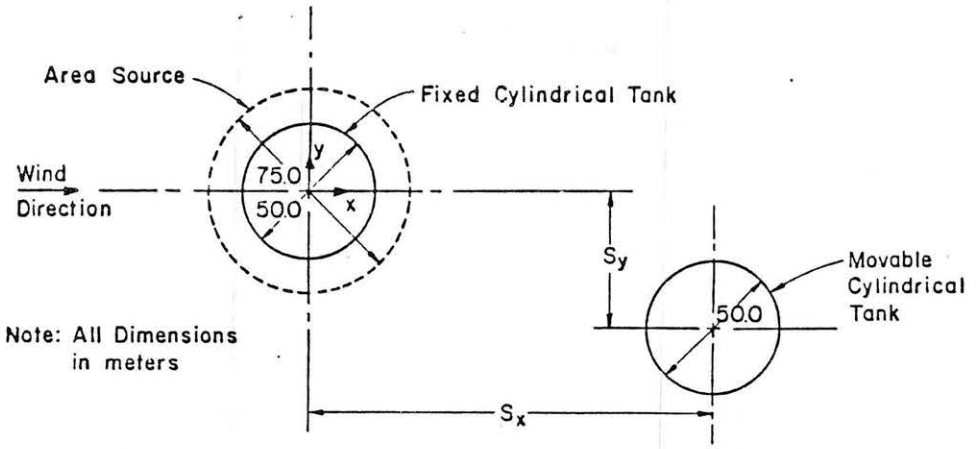

Note: All Dimensions in meters

Configuration	Displacement in x Direction S_x, meters	Displacement in y Direction S_y, meters
10	150.0	0.0
11	150.0	-50.0
12	250.0	0.0

Fig. 4.3-1c Concentration Measurement Locations and Configuration 1 - 22 Spill Arrangement

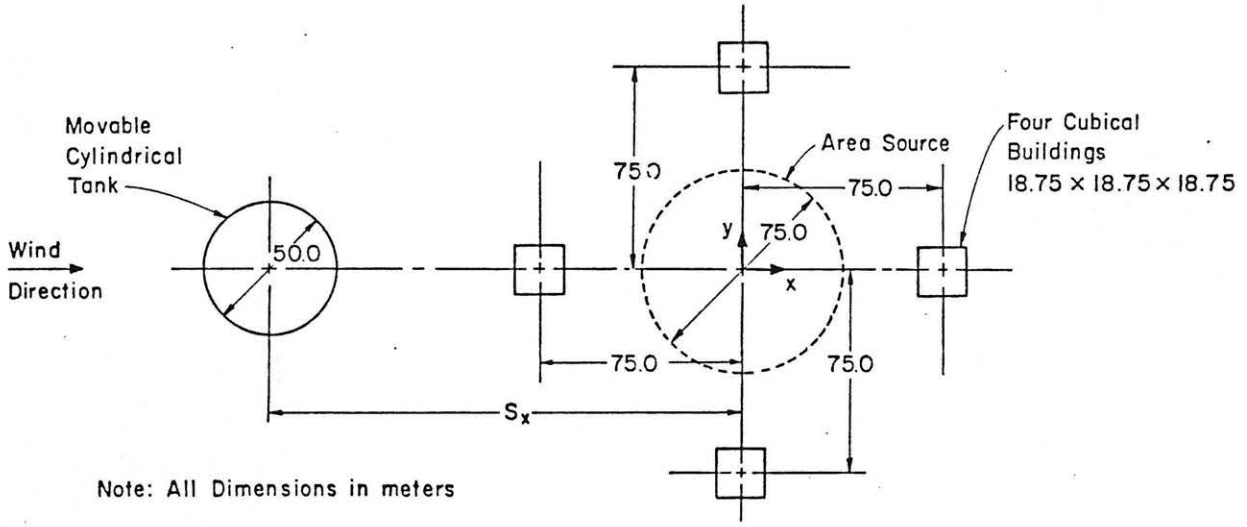

Configuration	Displacement in x Direction S_x, meters
13	-250.0
14	-150.0
15	0.0
16	150.0
17	250.0

Fig. 4.3-1d Concentration Measurement Locations and Configuration 1 - 22 Spill Arrangement

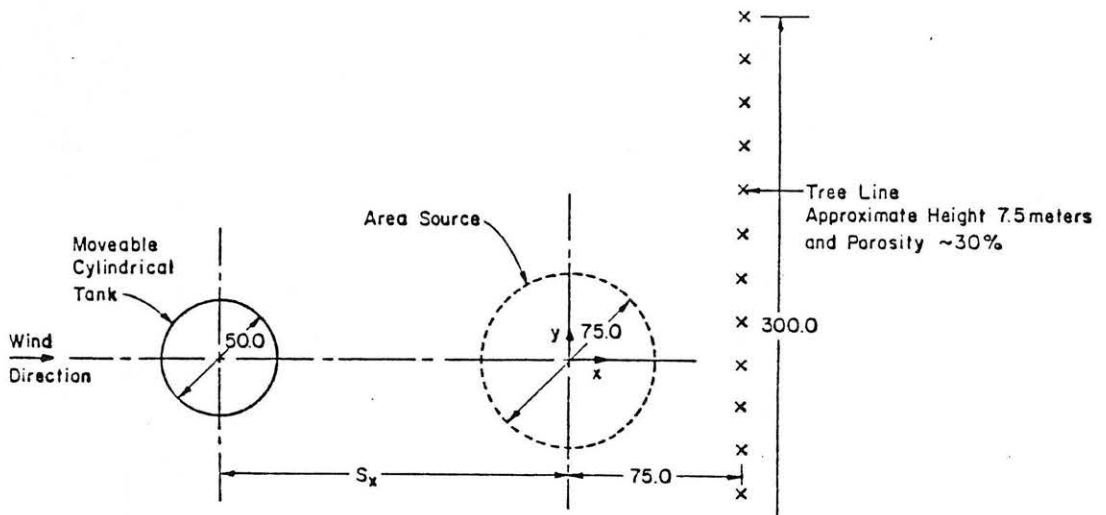

Configuration	Displacement in x Direction S_x, meters
18	-250.0
19	-150.0
20	0.0
21	150.0
22	250.0

Fig. 4.3-1e Concentration Measurement Locations and Configuration 1 - 22 Spill Arrangement

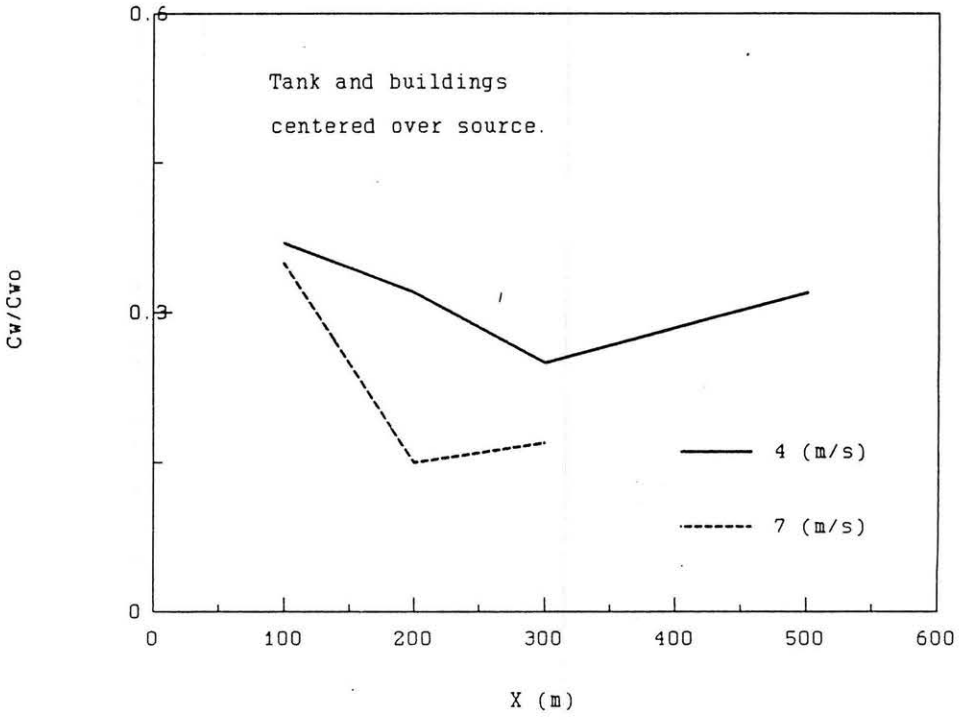

Fig. 4.3-2 Peak Concentration Ratio vs Downwind Distance, Configuration 15 , U = 4 and 7 m/sec

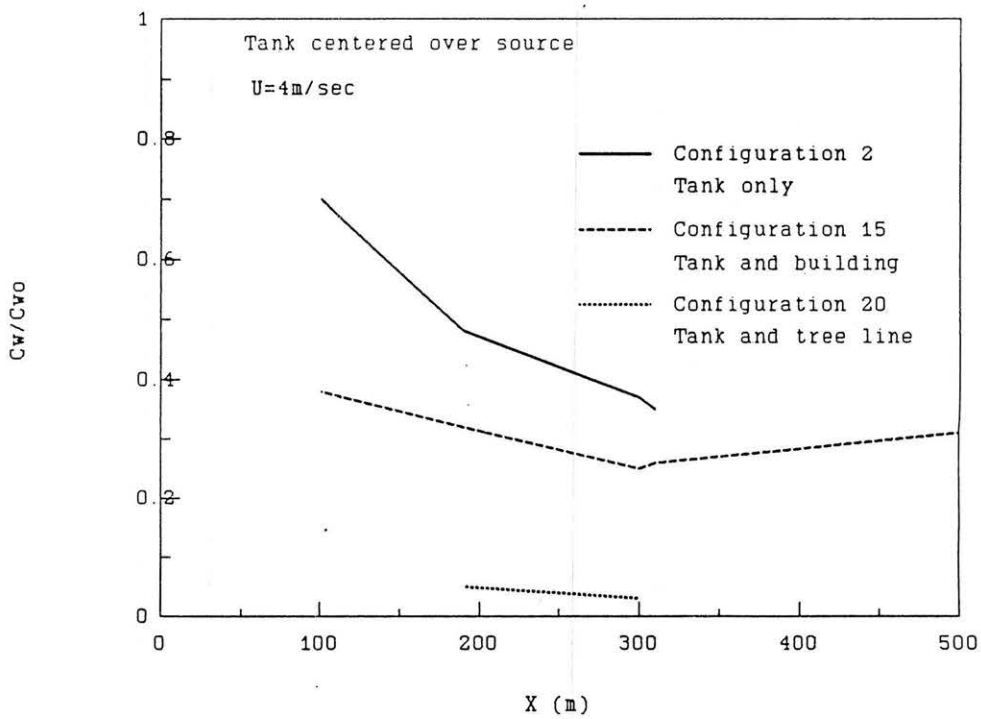

Fig. 4.3-3 Peak Concentration Ratio vs Downwind Distance, Configurations 2, 15 and 20

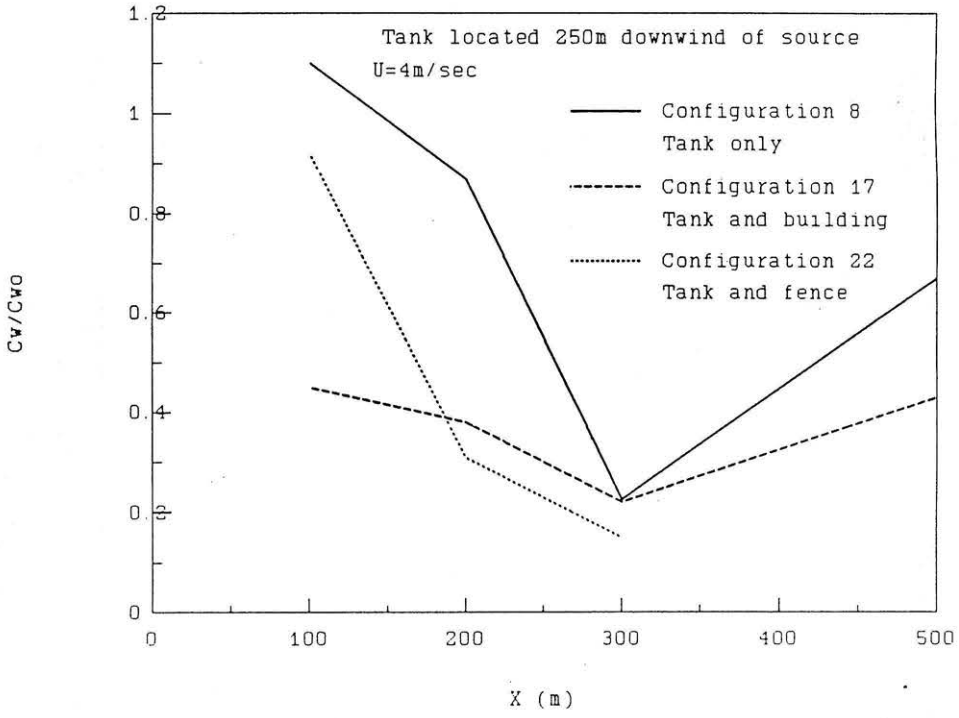

Fig. 4.3-4 Peak Concentration Ratio vs Downwind Distance, Configurations 8, 17 and 22

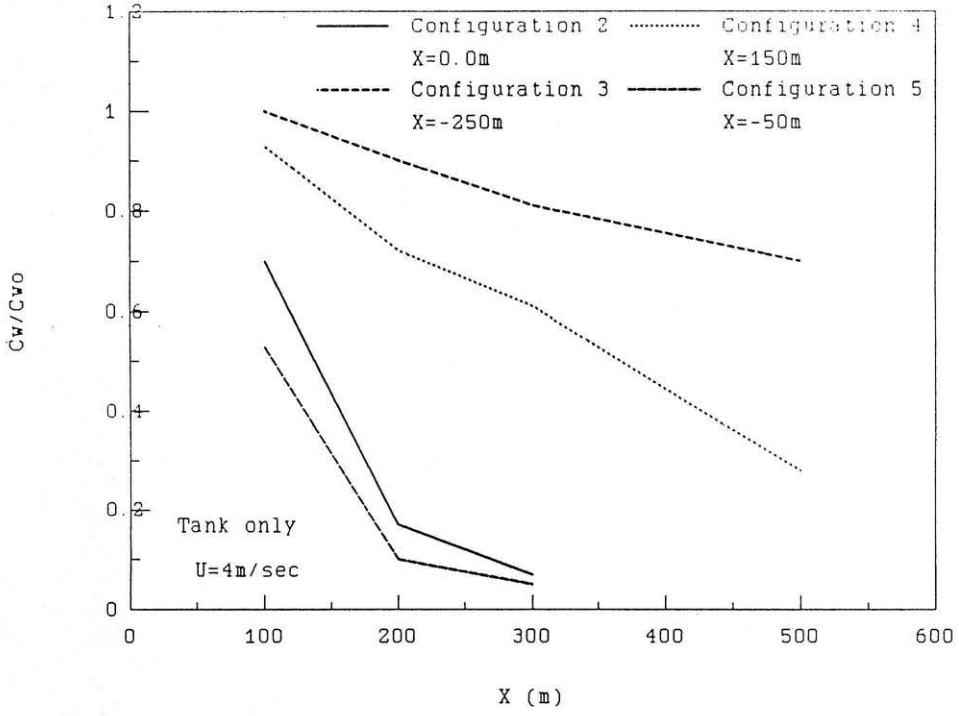

Fig. 4.3-5a Peak Concentration Ratio vs Downwind Distance, Configurations 2, 3, 4 and 5

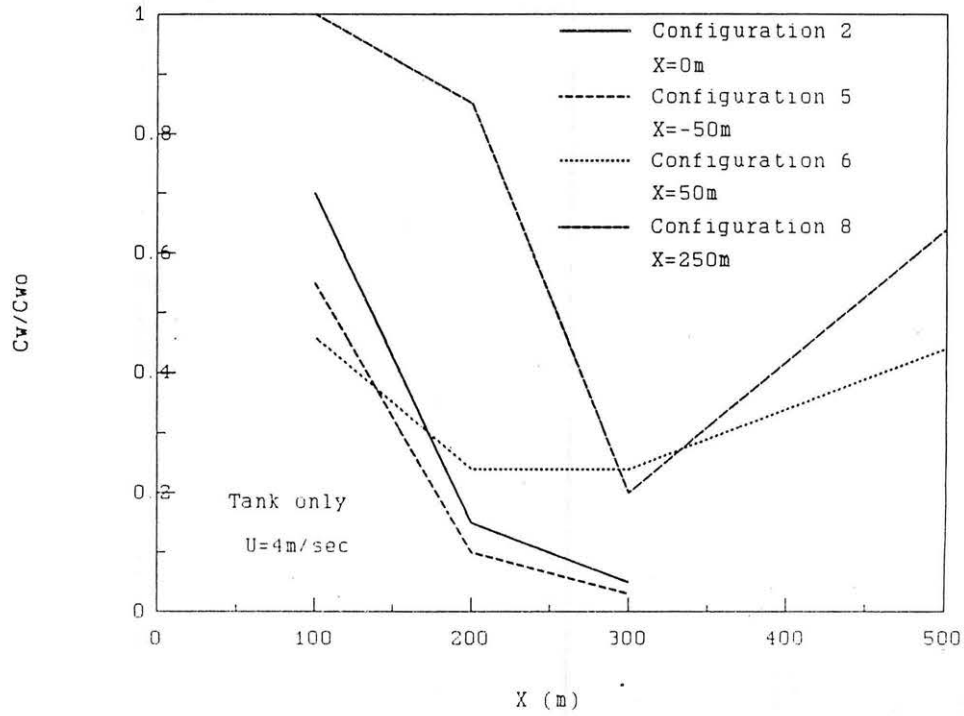

Fig. 4.3-5b Peak Concentration Ratio vs Downwind Distance, Configurations 2, 5, 6, and 8

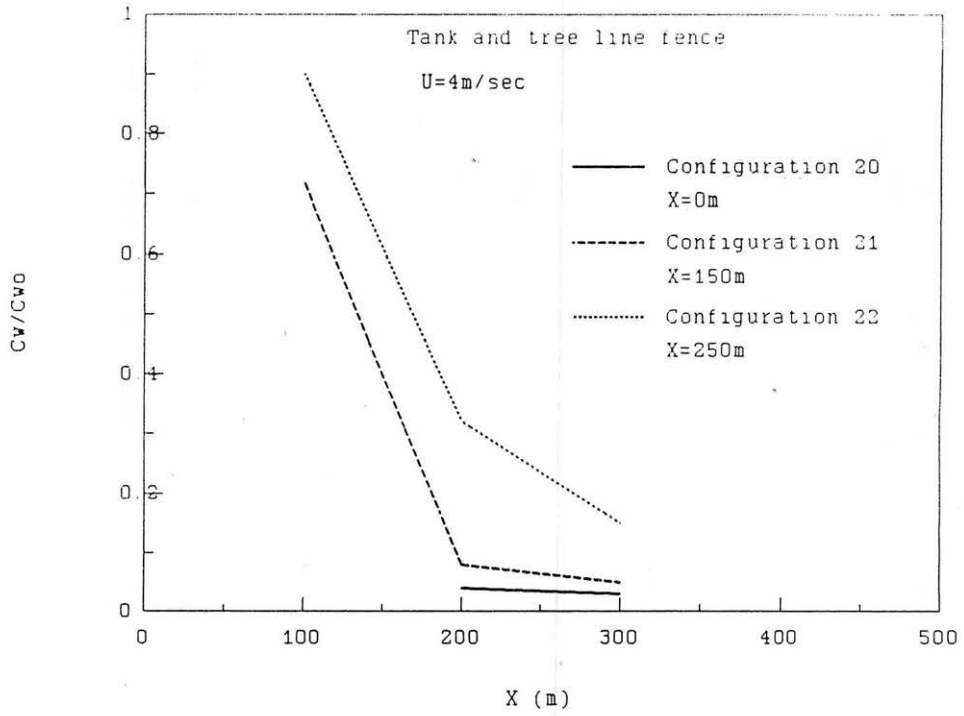

Fig. 4.3-6 Peak Concentration Ratio vs Downwind Distance, Configurations 20, 21, and 22

4.4 "Accelerated Dilution of Liquefied Natural Gas Plumes with Fences and Vortex Generators," Kothari, and Meroney, 1982

Experiment Configuration:

A wind-tunnel test program was conducted for dense gas dispersion over a 1:250 scale model with continuous releases from an LNG spill to determine the effects of fence and vortex generator vapor barriers. The experiments considered three simulated LNG spill rates (20, 30, and 40 cubic meters LNG/min), four wind speeds (4, 7, 9, and 12 m/sec), two barrier heights (5 and 10 m), three enclosure arrangements (Figure 4.4-2), and a solid fence or a vortex-spire barrier (Figures 4.4-3 and 4.4-4). A total of 204 tests were performed. Surface concentrations were measured over a grid ranging from 100 to 500 m downwind of the 75 m diameter spill pool (Figure 4.4-1).

Results of Comparison:

Ratios of centerline peak concentration with and without the barriers present were plotted versus downwind distance for each test case. Both fences and vortex generators produced smaller peak concentration ratios as wind speed increased (Figure 4.4-5); however, speeds above 7 m/sec produced similar levels of dilution (Frequently, the barriers were less efficient at 12 m/sec than at lower speeds, which may reflect a diminishing influence of gravity spreading on plume dynamics). Taller barriers (10 m) were also two times more effective than shorter barriers (5 m).

Solid fences diluted the gas cloud more effectively than the vortex spire arrangement; although in many cases the differences were minor (Figure 4.4-6). Fences placed directly around the spill area did not reduce peak concentrations as effectively as fences placed a bit farther away (Figure 4.4-7). Although the two-fence arrangement (Configuration 3) generally reduced peak concentrations the most, it often did not perform significantly different than the one-fence arrangement (Configuration 2).

Conclusions:

Solid fence and vortex-spire barriers reduced peak concentrations along the centerline of simulated LNG spills out to distances of 500 m (wake distances of 85 fence heights for the 5 m fence or 42.5 fence heights for the 10 m fence). Peak concentration ratios rose slowly from minimum values observed near 200 m. Apparently the peak concentration ratio must asymptote to one significantly beyond the end of the measurement domain used for these tests. (Note: Numerical calculations discussed in Section 5.2 suggest a possible return to no-fence concentrations at distances of about 200 fence heights downwind of the vapor barrier.) The fences were less effective at the lowest wind speed tested (4 m/sec); however, performance remained the same for winds speeds greater than 7 m/sec. Barrier performance varied directly with barrier

height for all configurations. The fences were more effective when placed about 1 spill diameter away from the spill pool.

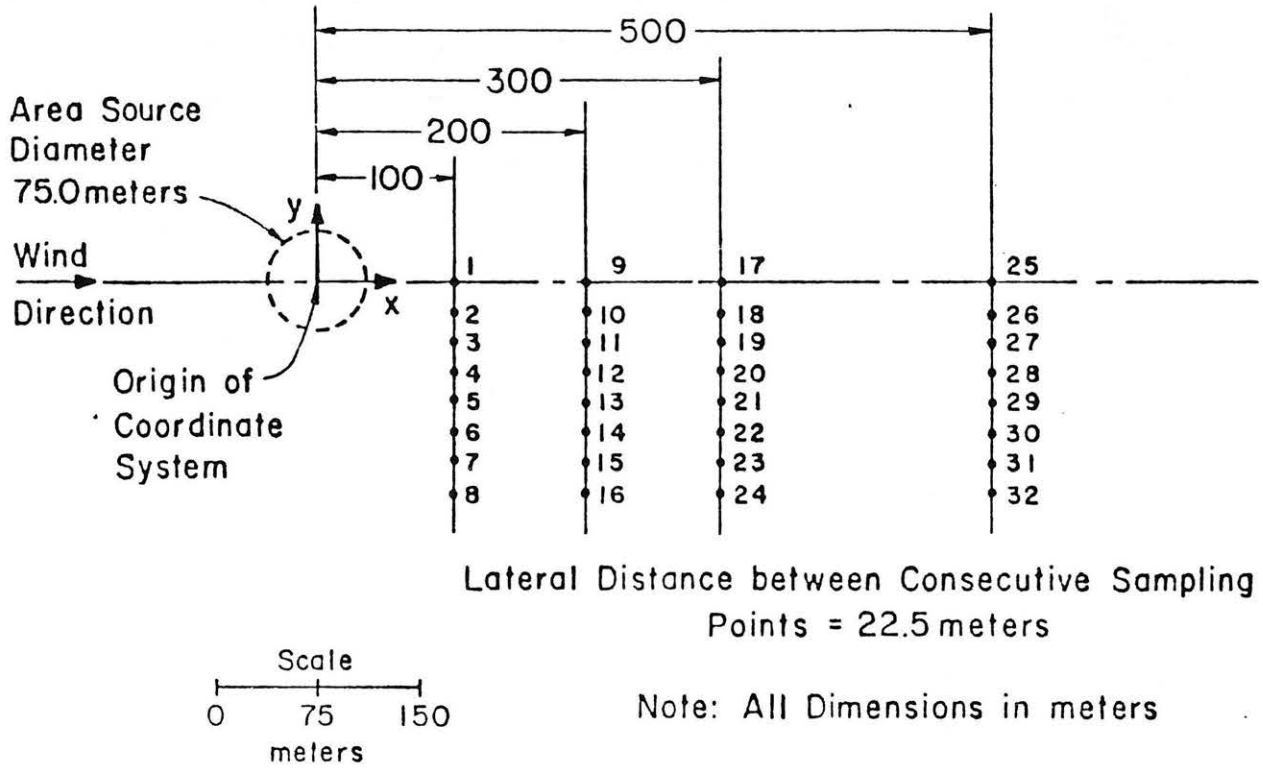

Fig. 4.4-1 Concentration Measurement Locations and Configuration 0 Spill Arrangement

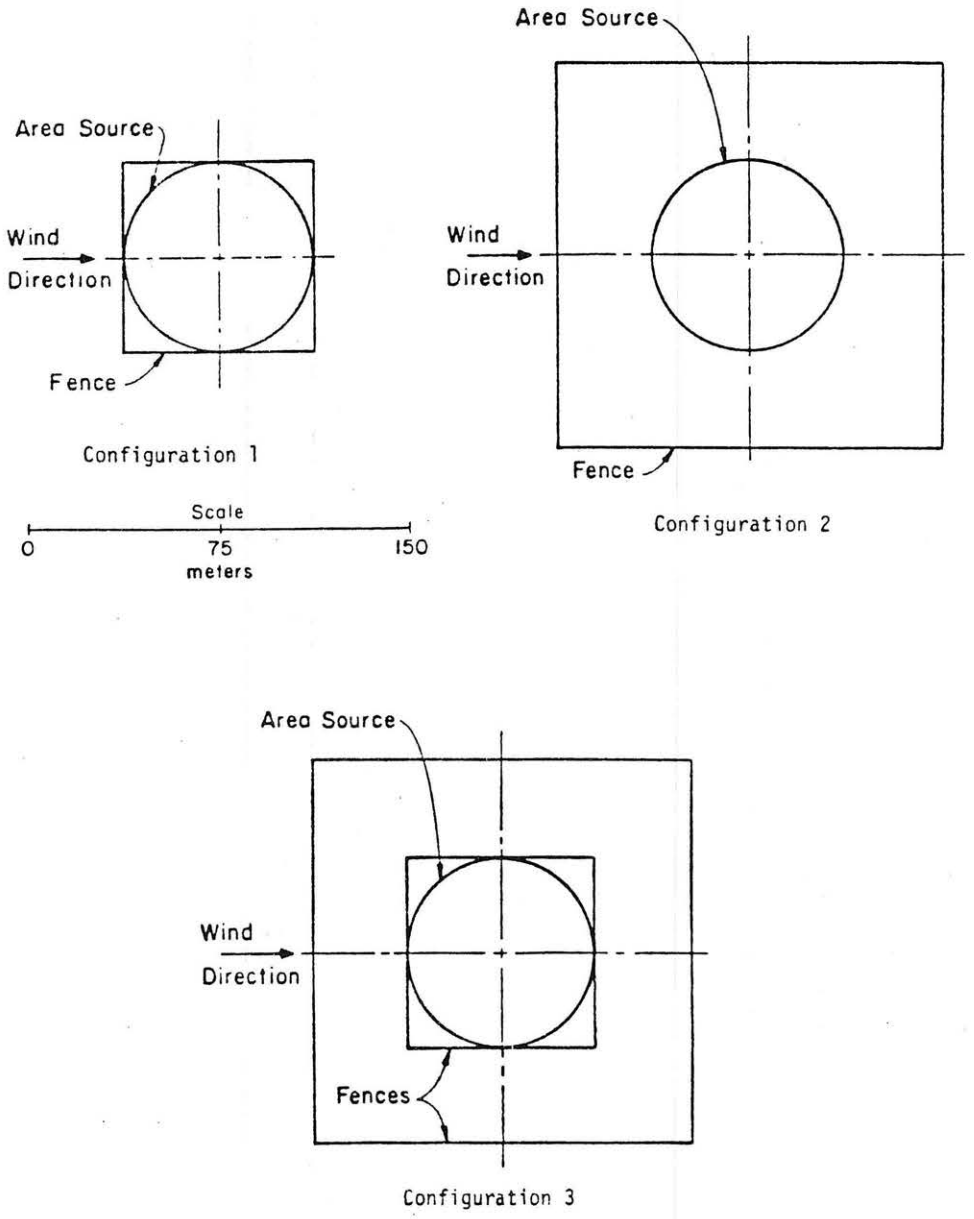

Fig. 4.4-2 Fence and Vortex Spire Configurations 1, 2, and 3

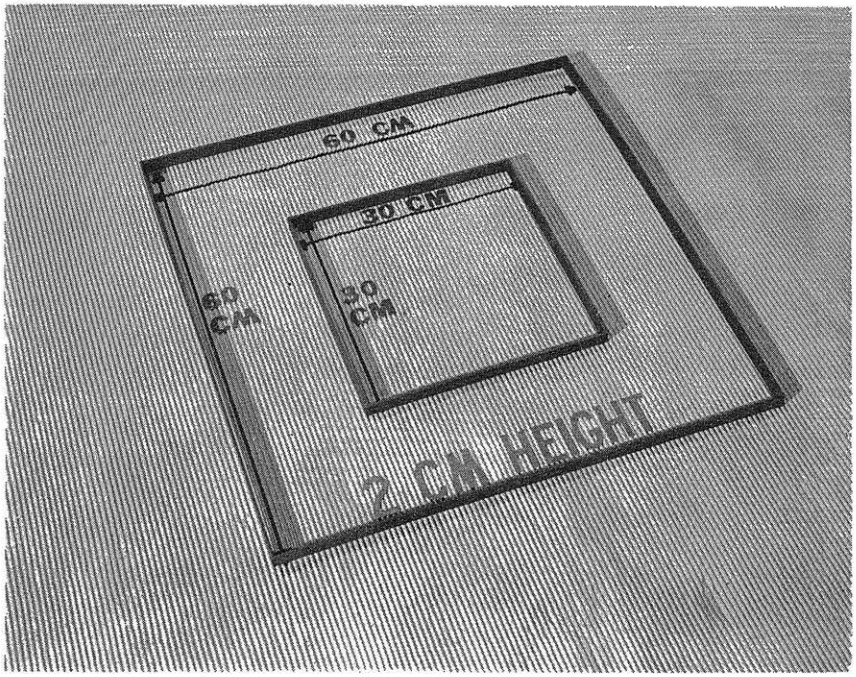

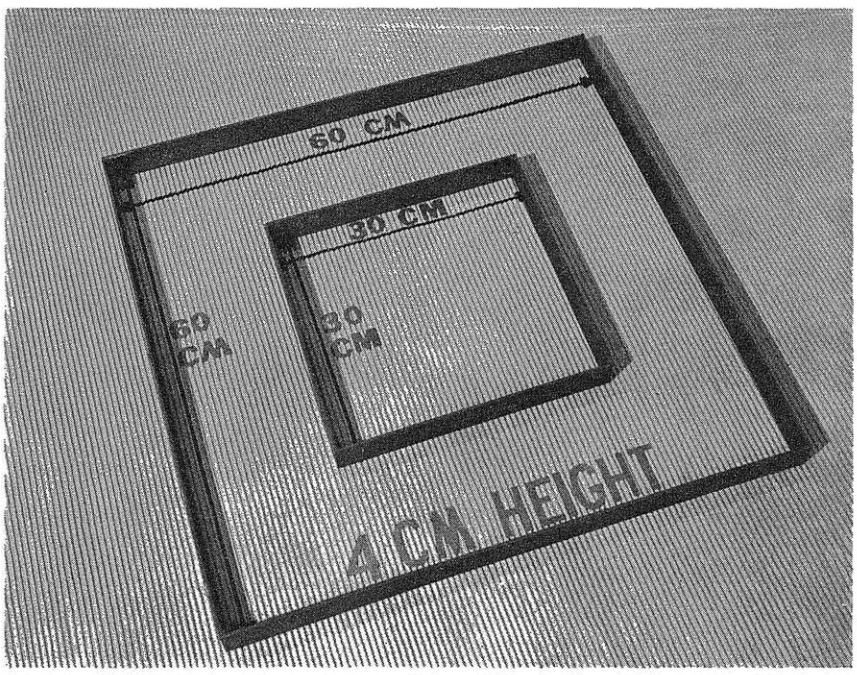

Fig. 4.3-3 Model Fence Enclosures

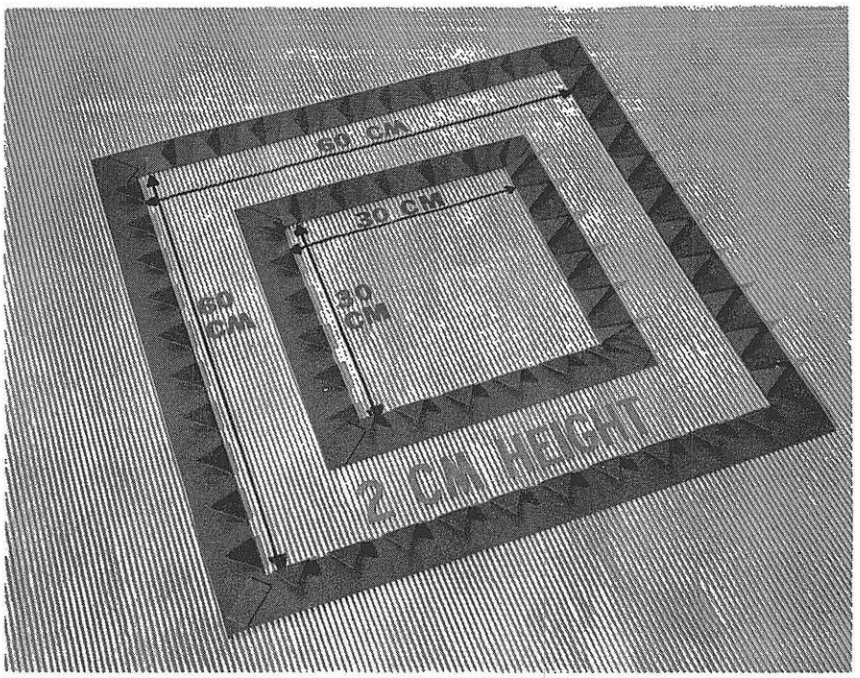

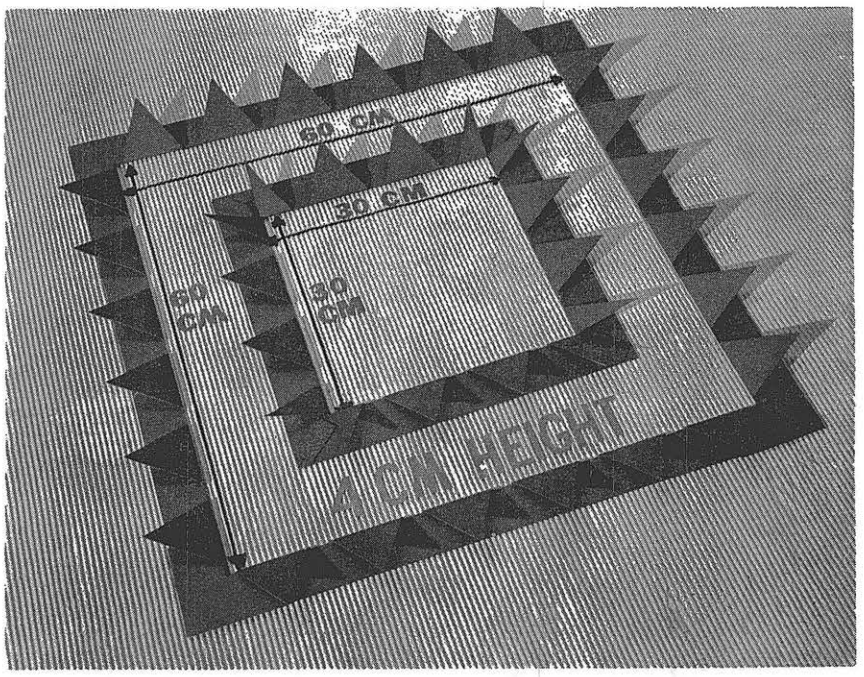

Fig. 4.3-4 Model Vortex Spire Enclosures

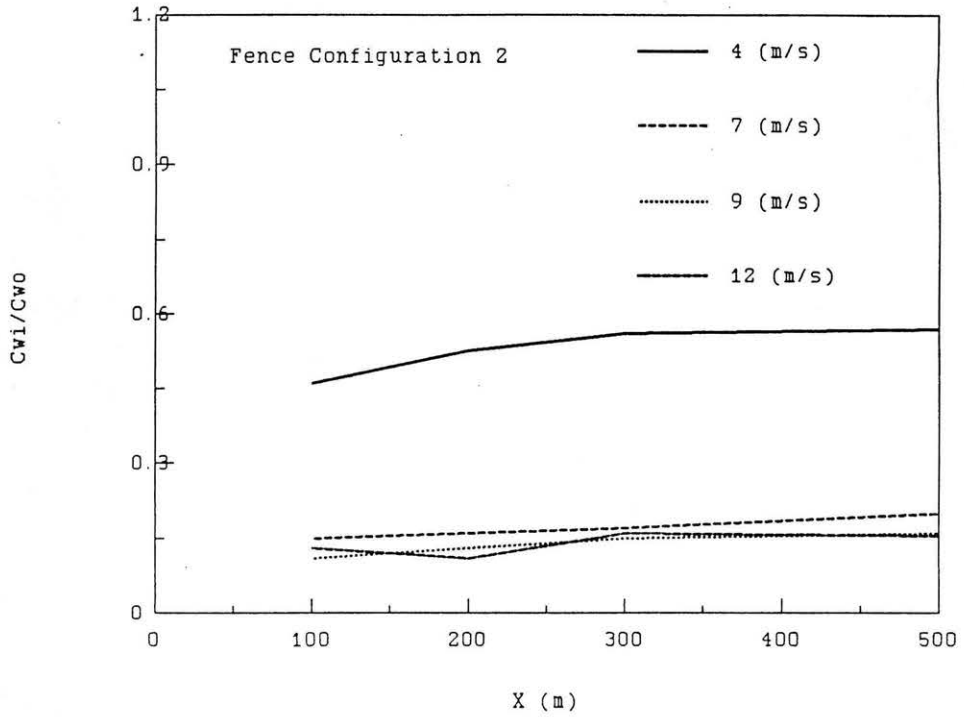

Fig. 4.4-5 Peak Concentration Ratio vs Downwind Distance, Q = 20 m^3/min LNG, Fence Height = 10 m, Wind Speed = 4, 7, 9, and 12 m/sec

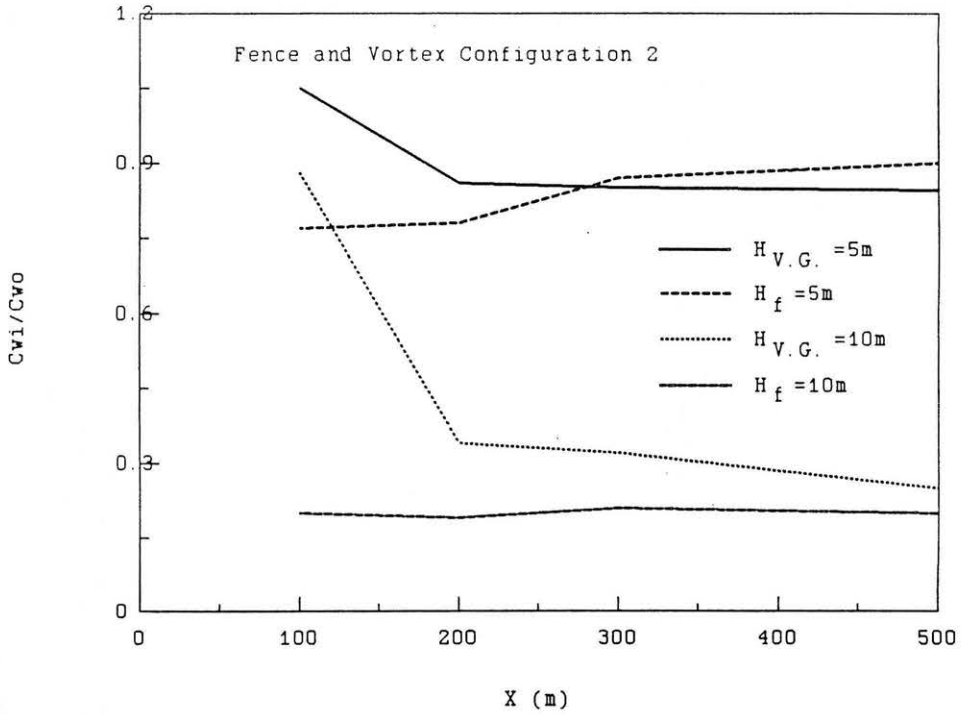

Fig. 4.4-6 Peak Concentration Ratio vs Downwind Distance, Q = 20 m^3/min LNG, Fence Heights = 5 and 10 m, Wind Speed = 4 m/sec, Fences and Vortex Spires

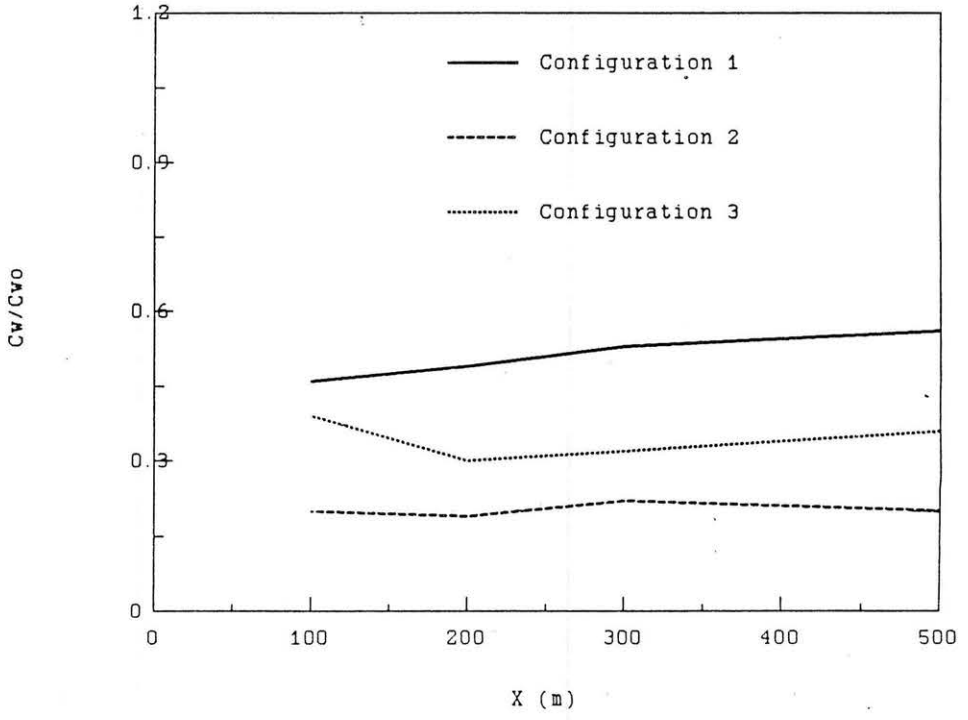

Fig. 4.4-7 Peak Concentration Ratio vs Downwind Distance, Q = 20 m^3/min LNG, Fence Height = 10 m, Wind Speed = 4 m/sec, Configurations 1, 2, and 3